The Center for Night Vision and Electro-Optics

OPTOELECTRONIC WORKSHOPS

X

FEMTOSECOND TIME-RESOLVED SPECTROSCOPY

November 3, 1988

sponsored jointly by

ARO-URI Center for Opto-Electronic Systems Research
The Institute of Optics, University of Rochester

2

UNCLASSIFIED
SECURITY CLASSIFICATION OF THIS PAGE

REPORT DOCUMENTATION PAGE

1a. REPORT SECURITY CLASSIFICATION Unclassified	1b. RESTRICTIVE MARKINGS
2a. SECURITY CLASSIFICATION AUTHORITY	3. DISTRIBUTION / AVAILABILITY OF REPORT Approved for public release; distribution unlimited.
2b. DECLASSIFICATION / DOWNGRADING SCHEDULE	
4. PERFORMING ORGANIZATION REPORT NUMBER(S)	5. MONITORING ORGANIZATION REPORT NUMBER(S) ARO 24626.78-PH-UIR
6a. NAME OF PERFORMING ORGANIZATION University of Rochester 6b. OFFICE SYMBOL (If applicable)	7a. NAME OF MONITORING ORGANIZATION U. S. Army Research Office
6c. ADDRESS (City, State, and ZIP Code) The Insitute of Optics Rochester, NY 14627	7b. ADDRESS (City, State, and ZIP Code) P. O. Box 12211 Research Triangle Park, NC 27709-2211
8a. NAME OF FUNDING / SPONSORING ORGANIZATION U. S. Army Research Office 8b. OFFICE SYMBOL (If applicable)	9. PROCUREMENT INSTRUMENT IDENTIFICATION NUMBER DAAL03-86-K-0173
8c. ADDRESS (City, State, and ZIP Code) P. O. Box 12211 Research Triangle Park, NC 27709-2211	10. SOURCE OF FUNDING NUMBERS PROGRAM ELEMENT NO. / PROJECT NO. / TASK NO. / WORK UNIT ACCESSION NO.

11. TITLE (Include Security Classification)
Optoelectronic Workshop X: Femtosecond Time-Resolved Spectoscopy

12. PERSONAL AUTHOR(S)
Ian Walmsley

13a. TYPE OF REPORT	13b. TIME COVERED	14. DATE OF REPORT (Year, Month, Day)	15. PAGE COUNT
Technical	FROM _____ TO _____	November 3, 1988	

16. SUPPLEMENTARY NOTATION
The view, opinions and/or findings contained in this report are those of the author(s) and should not be construed as an official Department of the Army position, policy, or decision, unless so designated by other documentation.

17. COSATI CODES		
FIELD	GROUP	SUB-GROUP

18. SUBJECT TERMS (Continue on reverse if necessary and identify by block number)
Workshop; femtosecond; spectoscopy

19. ABSTRACT (Continue on reverse if necessary and identify by block number)

This workshop on "Femtosecond Time-Resolved Spectoscopy" represents the tenth of a series of intensive academic/ government interactions in the field of advanced electro-optics, as part of the Army sponsored University Research Initiative. By documenting the associated technology status and dialogue it is hoped that this baseline will serve all interested parties towards providing a solution to high priority Army requirements. Responsible for program and program execution are Dr. Nicholas George, University of Rochester (ARO-URI) and Dr. Rudy Buser, NVEOC.

20. DISTRIBUTION / AVAILABILITY OF ABSTRACT	21. ABSTRACT SECURITY CLASSIFICATION
☐ UNCLASSIFIED/UNLIMITED ☐ SAME AS RPT. ☐ DTIC USERS	Unclassified
22a. NAME OF RESPONSIBLE INDIVIDUAL Nicholas George	22b. TELEPHONE (Include Area Code) 716-275-2417 / 22c. OFFICE SYMBOL

DD FORM 1473, 84 MAR — 83 APR edition may be used until exhausted. All other editions are obsolete.

SECURITY CLASSIFICATION OF THIS PAGE
UNCLASSIFIED

The Center for Night Vision and Electro-Optics

OPTOELECTRONIC WORKSHOPS

X

FEMTOSECOND TIME-RESOLVED SPECTROSCOPY

November 3, 1988

sponsored jointly by

ARO-URI Center for Opto-Electronic Systems Research
The Institute of Optics, University of Rochester

OPTOELECTRONIC WORKSHOP

ON

FEMTOSECOND TIME-RESOLVED SPECTROSCOPY

Organizer: ARO-URI-University of Rochester
and Center for Night Vision and Electro-Optics

1. INTRODUCTION

2. SUMMARY -- INCLUDING FOLLOW-UP

3. VIEWGRAPH PRESENTATIONS

   A. Center for Opto-Electronic Systems Research
      Organizer -- Ian Walmsley

      Femtosecond Time-Resolved Spectroscopy
      Ian Walmsley

      Experimental Techniques for Femtosecond Spectroscpy
      Iam Walmsley

      Femtosecond Relaxation Processes in Semiconductors
      Ian Walmsley

      Femtosecond Spectroscopy of Large Molecules
      Ian Walmsley

   B. Center for Night Vision and Electro-Optics
      Organizer -- Edward Sharp

      Nonlinear Optics: Materials Research
      Edward Sharp

4. LIST OF REFERENCES

5. LIST OF ATTENDEES

6. DISTRIBUTION

1. INTRODUCTION

This workshop on "Femtosecond Time-Resolved Spectroscopy" represents the tenth of a series of intensive academic/ government interactions in the field of advanced electro-optics, as part of the Army sponsored University Research Initiative. By documenting the associated technology status and dialogue it is hoped that this baseline will serve all interested parties towards providing a solution to high priority Army requirements. Responsible for program and program execution are Dr. Nicholas George, University of Rochester (ARO-URI) and Dr. Rudy Buser, NVEOC.

2. SUMMARY AND FOLLOW-UP ACTIONS

Dr. Ed Sharp opened the meeting with a few preliminary remarks on the NVEOC mission, and how his group's work on optical materials and phase conjugation fit into the scheme.

Dr. Sharp then presented a talk on the development of materials for nonlinear optics. The characterization of these materials was highlighted, especially with regard to the use of time-resolved spectroscopy to obtain important material parameters.

Dr. Ian Walmsley then discussed the research at the Institute of Optics in ultrafast time-resolved spectroscopy. This involves developing new laser sources and new spectroscopic techniques, as well as their application to other research projects.

A tour of the NVEOC laboratory facilities followed, with demonstrations of new effects in phase conjugation by Dr. Greg Salamo and measurement of materials parameters by Dr. Ed Sharp. This was preceded by a discussion of both group's work and the facilities available to and the interests of the participants.

The overlap of interests between the University and the Laboratory was not large in terms of finding common ground for collaborative work. However it was thought to be a worthwhile interaction because it allowed both sides to expand their horizons of possible techniques and applications.

One possible area of mutual interest is the problem of charge transport in liquid crystal molecules. The large dipole moments that are possible in these materials depends on the ability of electrons to move rapidly along the polymer chain. Time-resolved spectroscopy might be used as a method of measuring the rate at which this occurs. Keywords: Electrooptics, Femtosecond time; Workshops; Relaxation Time. (jhd)

CENTER FOR OPTO-ELECTRONIC SYSTEMS RESEARCH
FEMTOSECOND TIME-RESOLVED SPECTROSCOPY

Research in Femtosecond Time-Resolved Spectroscopy

I.A. Walmsley
The Institute of Optics
University of Rochester
Rochester NY 14627

-Development of new sources and amplifiers for ultrashort light pulses.

-Application to fundamental processes and potential device technologies.

1. Femtosecond Light Sources

- Lasers which produce extremely short (~20fs) light pulses are required for:
    - time-resolved spectroscopy
    - high-speed communications systems

- new sources
    - shorter pulses
    - tunable wavelengths

- research goals:
    - understand pulse-forming mechanisms
    - develop new sources (esp. solid-state)

2. Current Status:

- Passively Modelocked Dye lasers: (shortest pulse duration; 20fs [Sleat, Finch & Sibbett 1988])

- Colliding Pulse Modelocked (CPM)

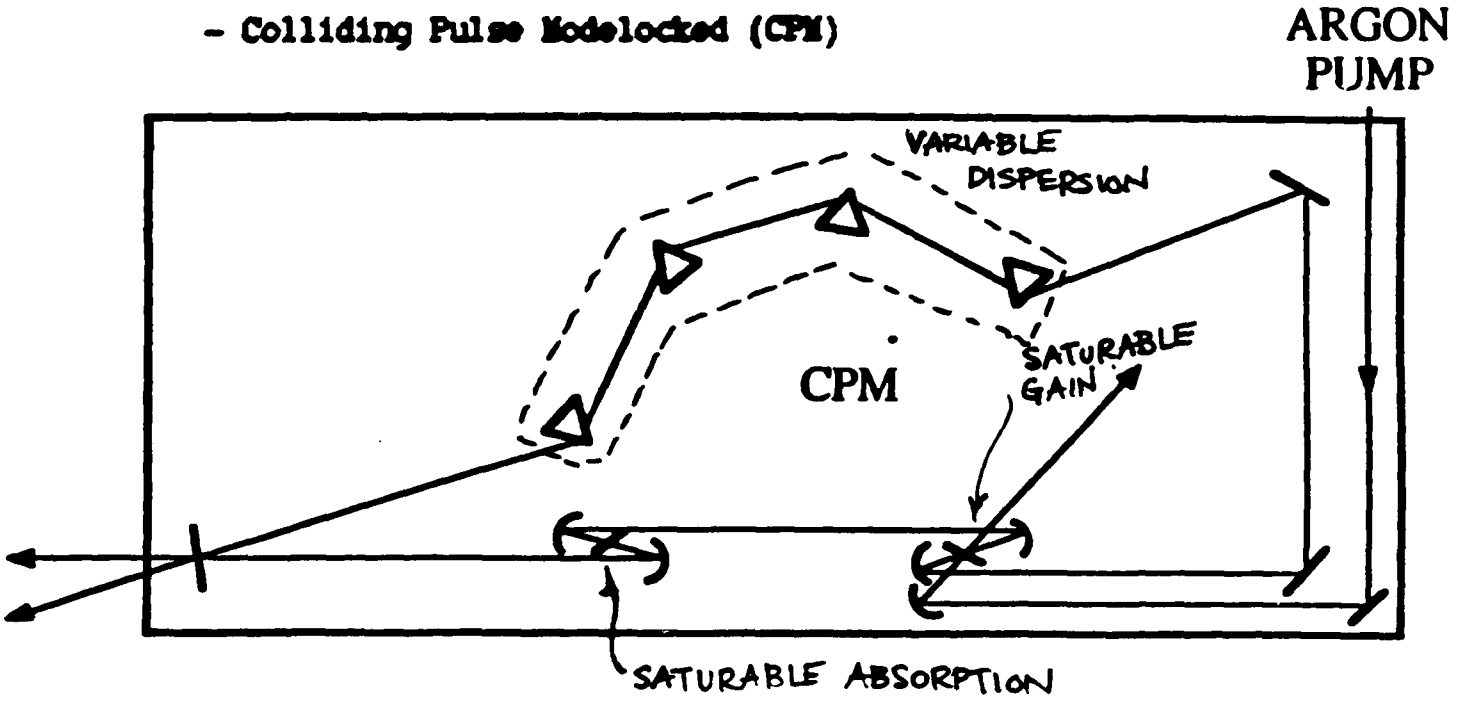

Key Features
- Saturable Gain
- Saturable Absorption
- Dispersive Nonlinearity
- Variable GVD

Theory: [Martinez, Fork & Gordon (1985),
Petrov, Rudolph & Wilhelmi (1987),
Avramopoulos, French, Williams, New & Taylor(1988)]

-Not tunable
-Liquid system
-Some regimes of operation not explained by theories

3. Laser output characterisation:

- Pulse shape and duration studied via intensity autocorrelation:

$$S_{Ac}(\tau) = \int_{-T}^{T} dt\ I(t)\, I(t+\tau)$$

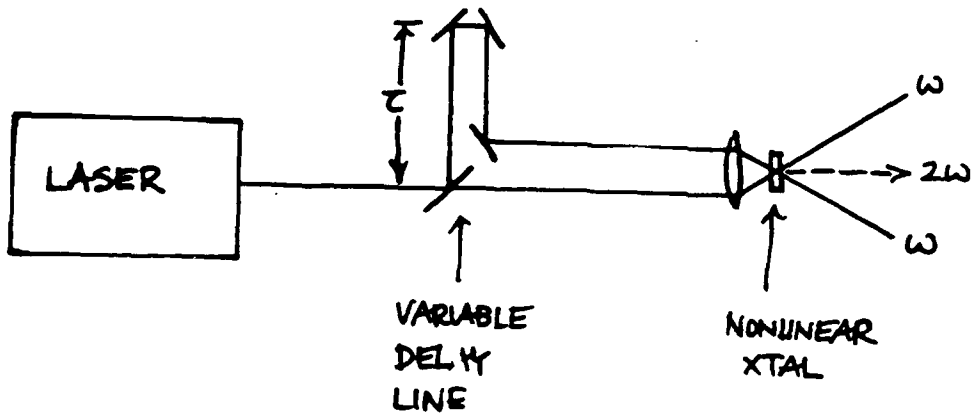

- Typical results:

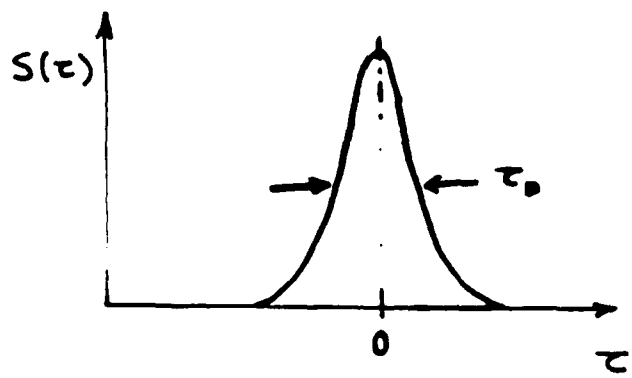

- τ_D related to pulse duration, assuming a pulse shape

4. Soliton-like pulses:
[Valdmanis, Fork & Gordon (1985)
Diels, Menders & Sallaber (1985)
Salin, Grangier, Roger & Bruns (1986)
Wise, Walmsley & Tang (1988)]

- stable, periodic pulse sequence

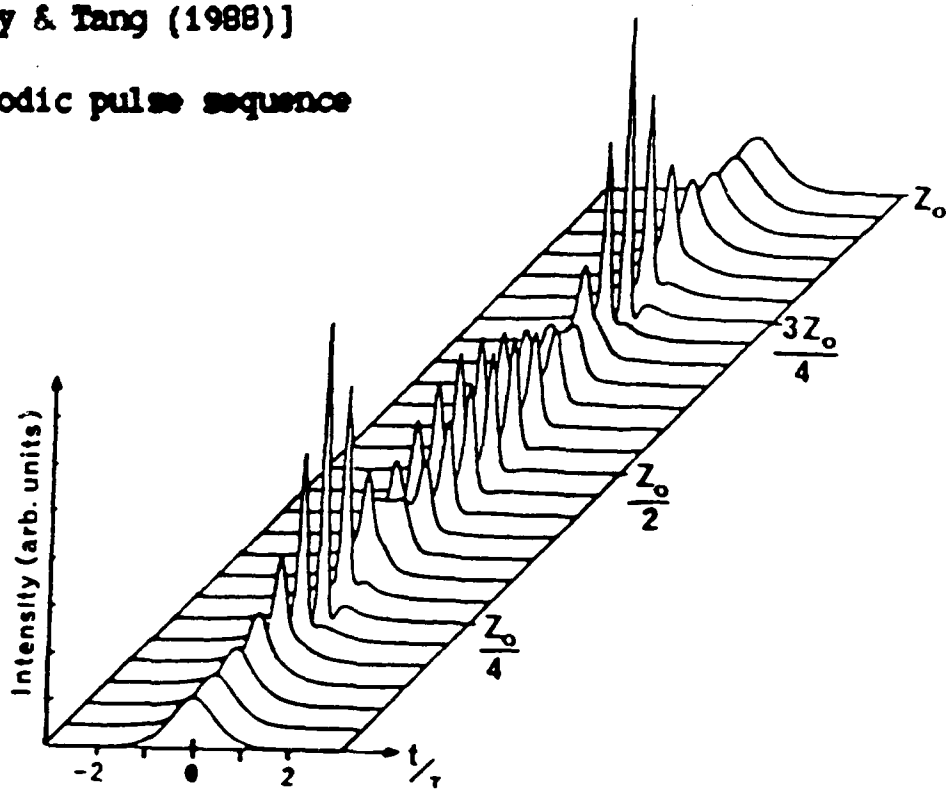

- laser has some characteristics of soliton-supporting media;
  - nonlinearity
  - dispersion

- in addition, there are also;
  - gain and loss mechanisms
  - non-continuous nonlinearity and dispersion

5. Concurrent soliton and dispersive wave:
[Wise, Valmsley & Tang (1988)]

- Laser output comprised of two parts:

N=3 soliton + usual "short" pulse

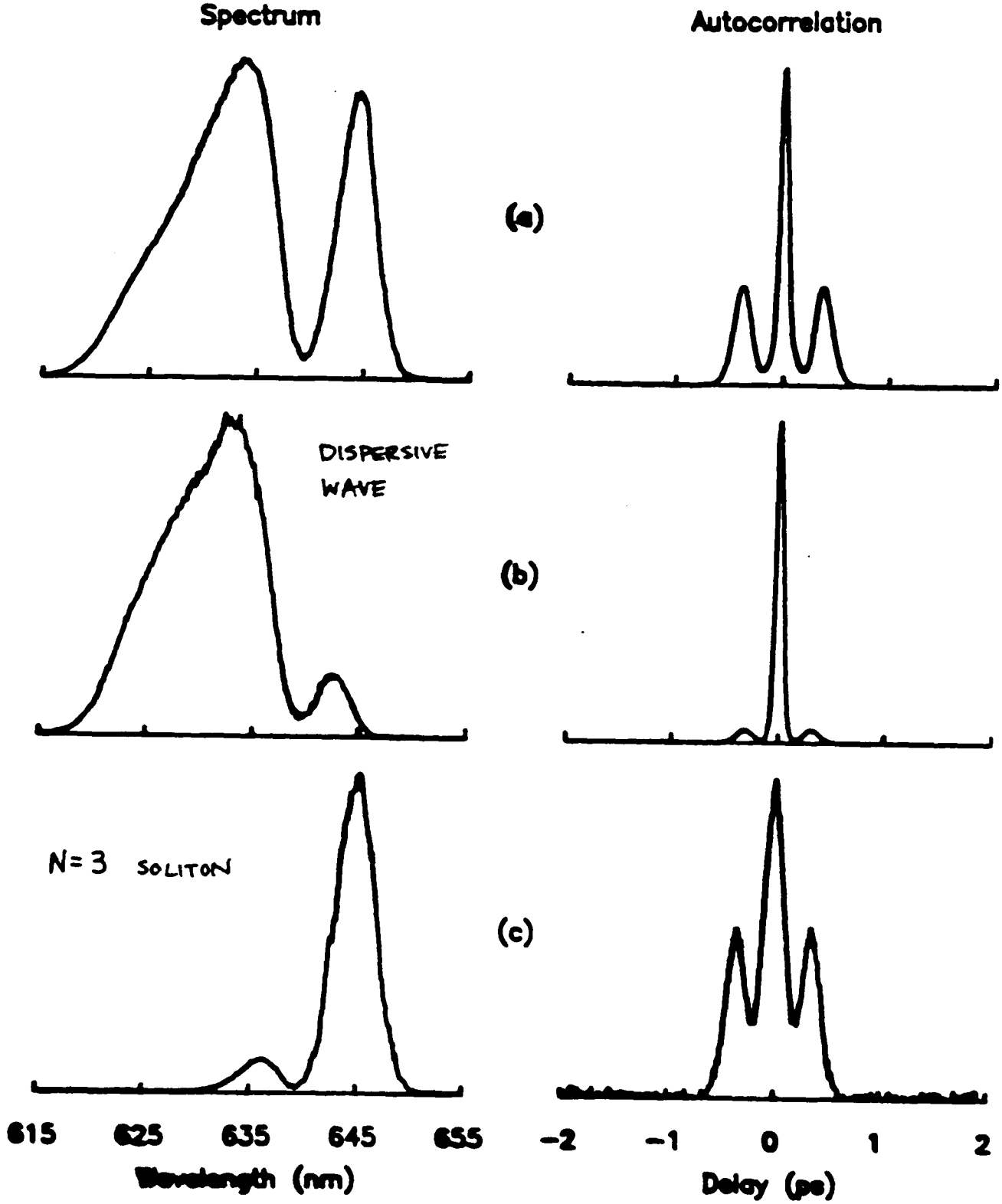

6. <u>Evidence for soliton-like pulses:</u>

- Soliton part of spectrum shows periodic modulation

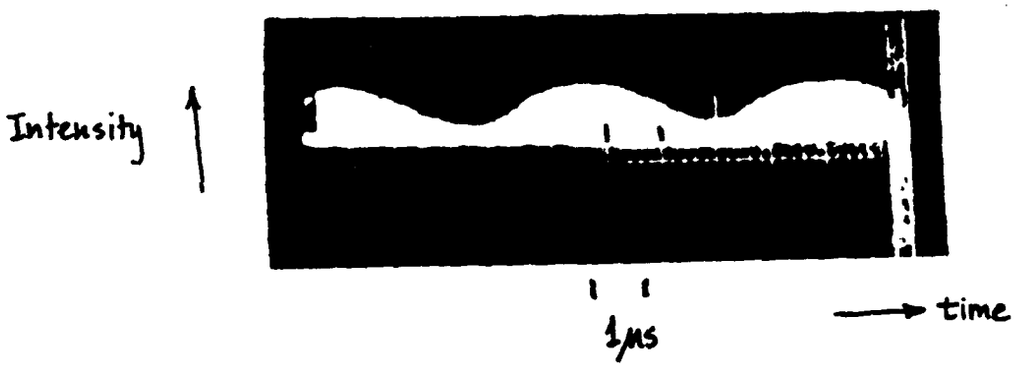

- Soliton period, τ, related to material dispersion

$$1/\tau = \frac{2\phi''}{0.3\pi\ \tau_p\ T}$$

T = CAVITY ROUND TRIP

$\phi'' = \partial\phi/\partial\omega$ = CAVITY/MATERIAL DISPERSION

- τ=5μs => ϕ''= -180,-250fs^2 => 3-5mm of quartz

- Inferred intracavity dispersion agrees with that estimated from the quartz prism sequence.

7. Effective zero-dispersion point:

- Both types of pulses can occur simultaneously at the zero-dispersion point ($\phi''=0$) of an optical fiber. [Vai & Menyuk (1988)]

- Introduce "effective zero-dispersion point" for CPM which delimits regime of stable, modelocked behaviour.

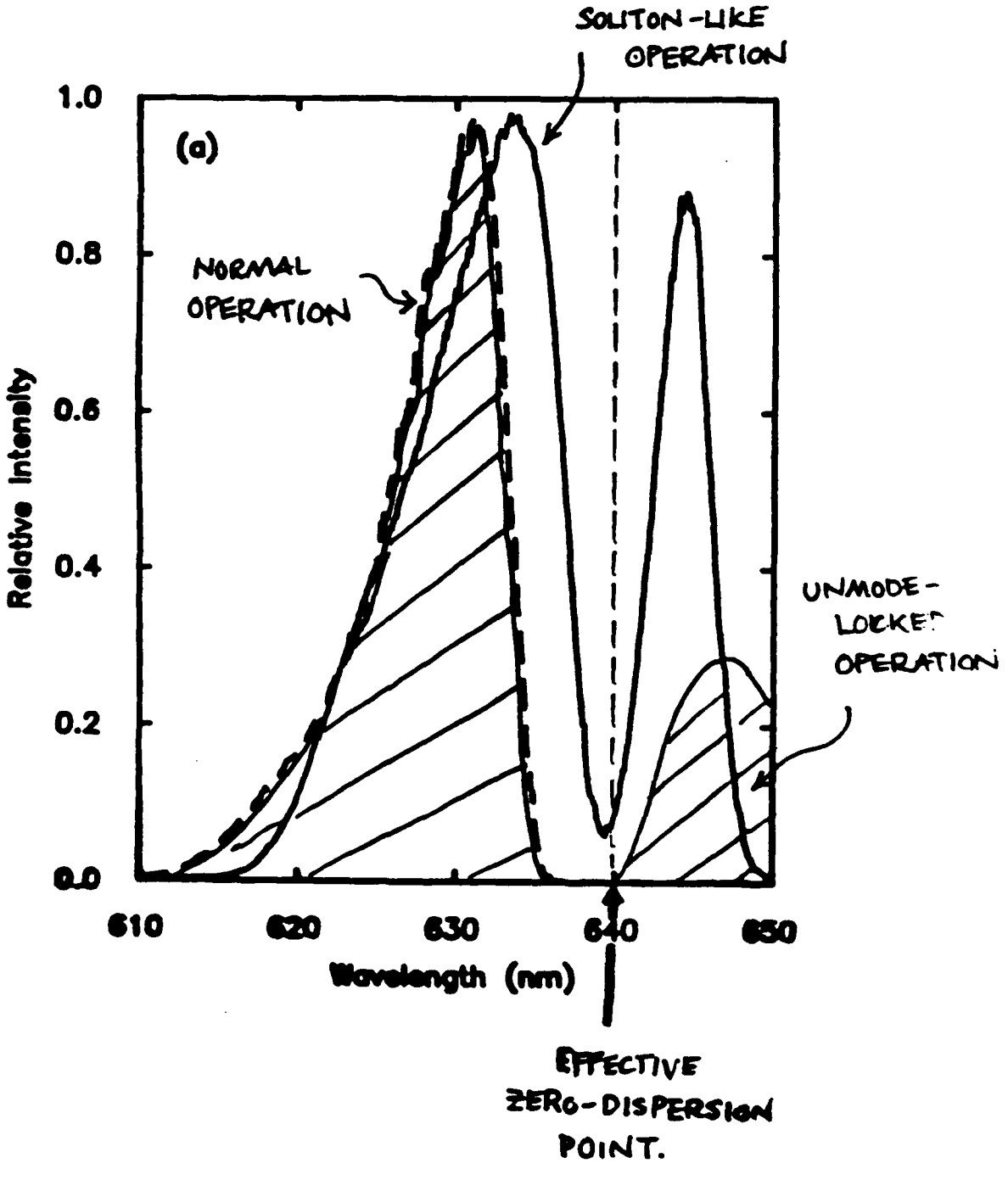

8. Relation between soliton and dispersive waves:

- Interferometric intensity autocorrelation

$$S_{IAC}(\tau) = S_{AC}(\tau) + 4\,\mathrm{Re}\int dt\; I(t)\,E(t)E(t+\tau)$$

↑

INTERFERENCE FRINGES

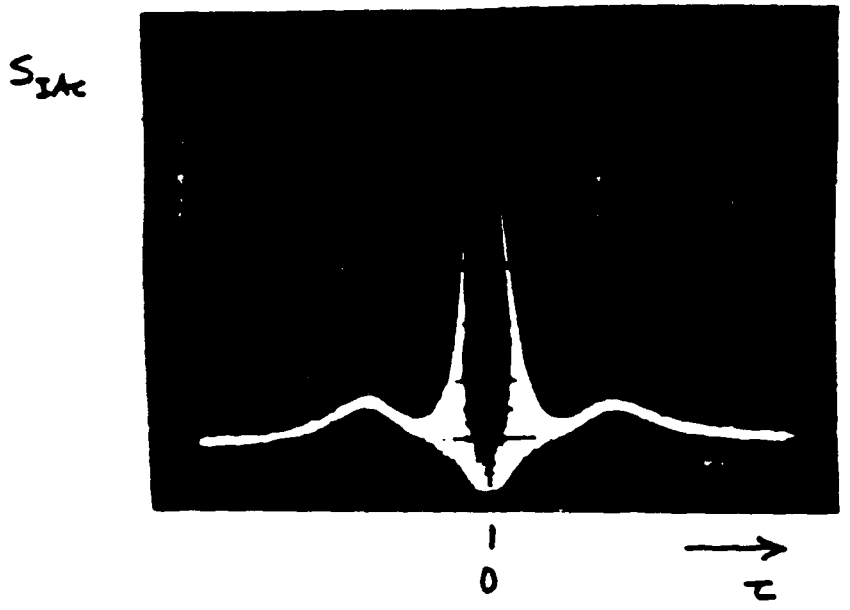

- lack of coherence between the dispersive parts and the soliton-like parts. Why?

9. Chirped solitons:

- $\Delta\zeta$ measured after extracavity prism sequence

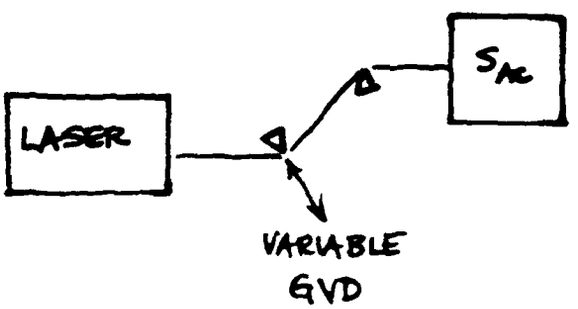

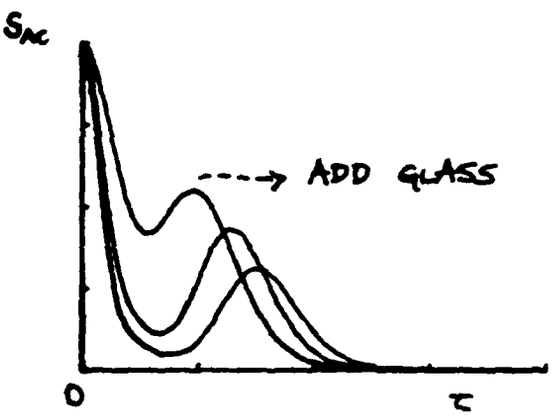

- Spectral windowing

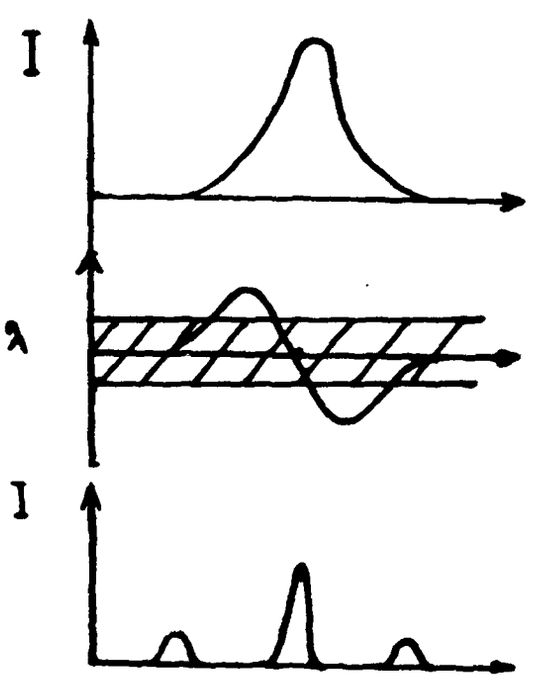

- Solitons are "chirped"

10. Current projects:

Problems;

- Current models fail to predict all types of soliton-like behaviour.

- Soliton-like regimes of operation have not been fully characterised.

Solutions;

- Determine the pulse electric field envelope using triple correlation and energy spectrum measurements.

$$- \; S_{TC}(\tau_1, \tau_2) = \int_{-T}^{T} dt \; I(t) I(t+\tau_1) I(t+\tau_2)$$

$$- \; S(\tau) = \int_{-T}^{T} dt \; E(t) E(t+\tau) = F.T.\{ |\tilde{E}(\omega)|^2 \}$$

$$- \; I(t) = |E(t)|^2 \quad ; \quad \boxed{E(t) = \mathcal{E}(t) e^{i\phi(t)}}$$

TIME-DEPENDENT PHASE

- Develop theory which includes molecular coherences and which retains high-order dispersion.

11. Summary:

- Soliton-like mechanisms are important in pulse shaping in the CPM. There are many different regimes in which solitons occur.

- The generation of soliton-like pulses in the CPM laser is not well understood, either via theory or experiment.

- There are significant differences from "usual" solitons (i.e. solutions to the nonlinear Schrodinger equation), due to the additional mechanisms (gain and loss) in the laser and the distributed nature of the nonlinearity and dispersion.

- There is a possibility for constructing passively-modelocked lasers at other wavelengths and using more robust materials by understanding and utilising these pulse shaping mechanisms.

High Repetition Rate Femtosecond Amplifier System

- New scheme for amplifying femtosecond pulses

- High-energy pulses (>10μJ)

-High-repetition rates (>30kHz)

-No cavity locking required

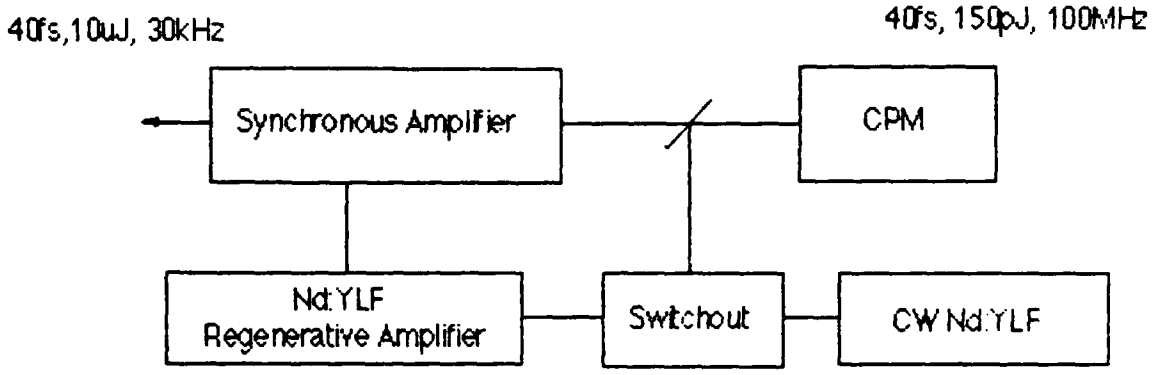

CENTER FOR OPTO-ELECTRONIC SYSTEMS RESEARCH

EXPERIMENTAL TECHNIQUES FOR FEMTOSECOND SPECTROSCOPY

Pump-Probe spectroscopy

Excitation: Pump pulse establishes medium excitation. Probe pulse is affected by medium excitation at some later time.

Measure: absorption, polarisation rotation, frequency upconversion of probe pulse

Result: Maps out time-development of medium excitation

Transmission-correlation spectroscopy

-measures transmitted intensity of both pump and probe pulses

-same information is returned as in a pump-probe experiment

-some technical advantages

Transmission-correlation spectroscopy

-measures same quantitites as pump-probe
-some technical advantages in this case

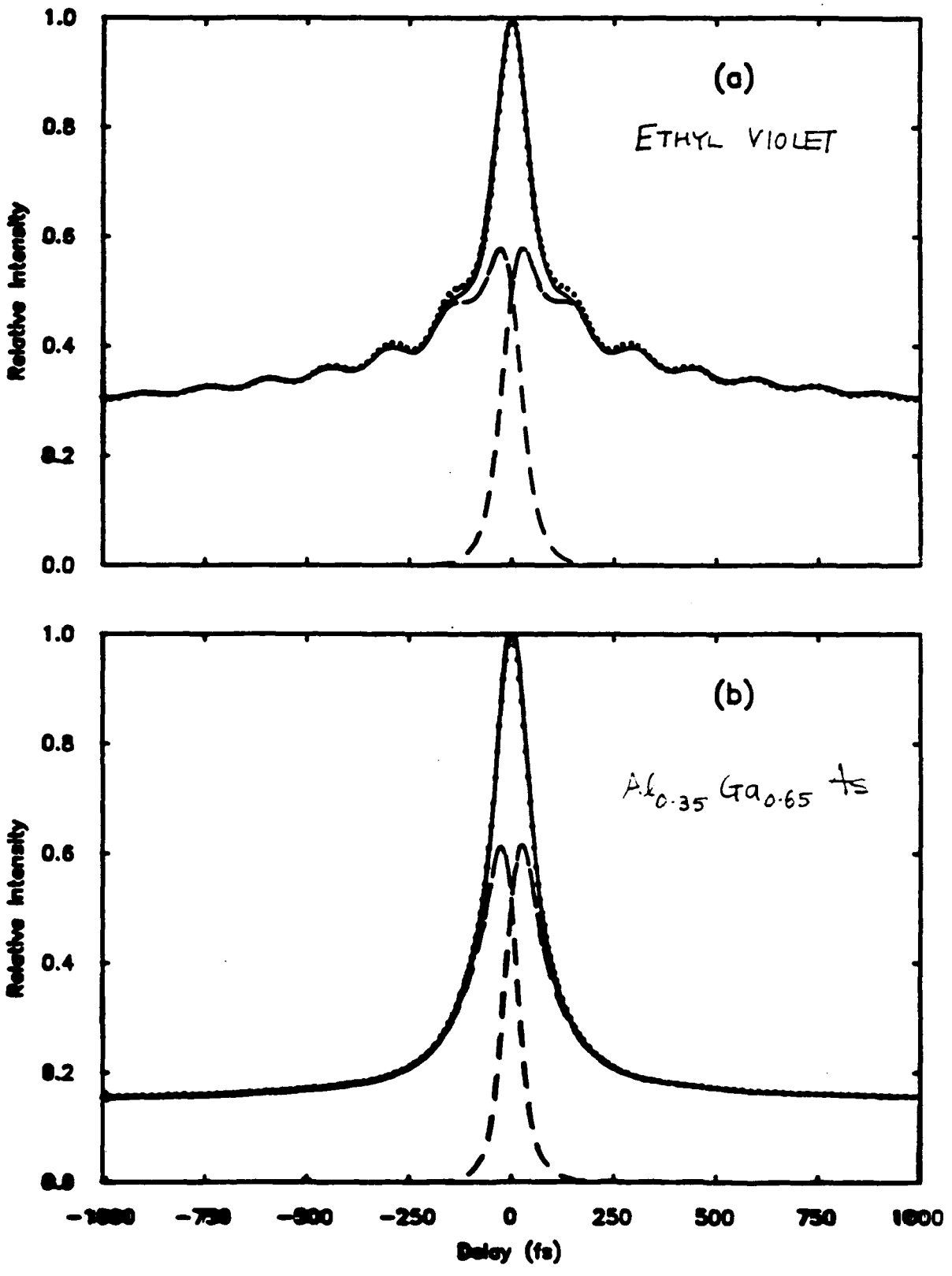

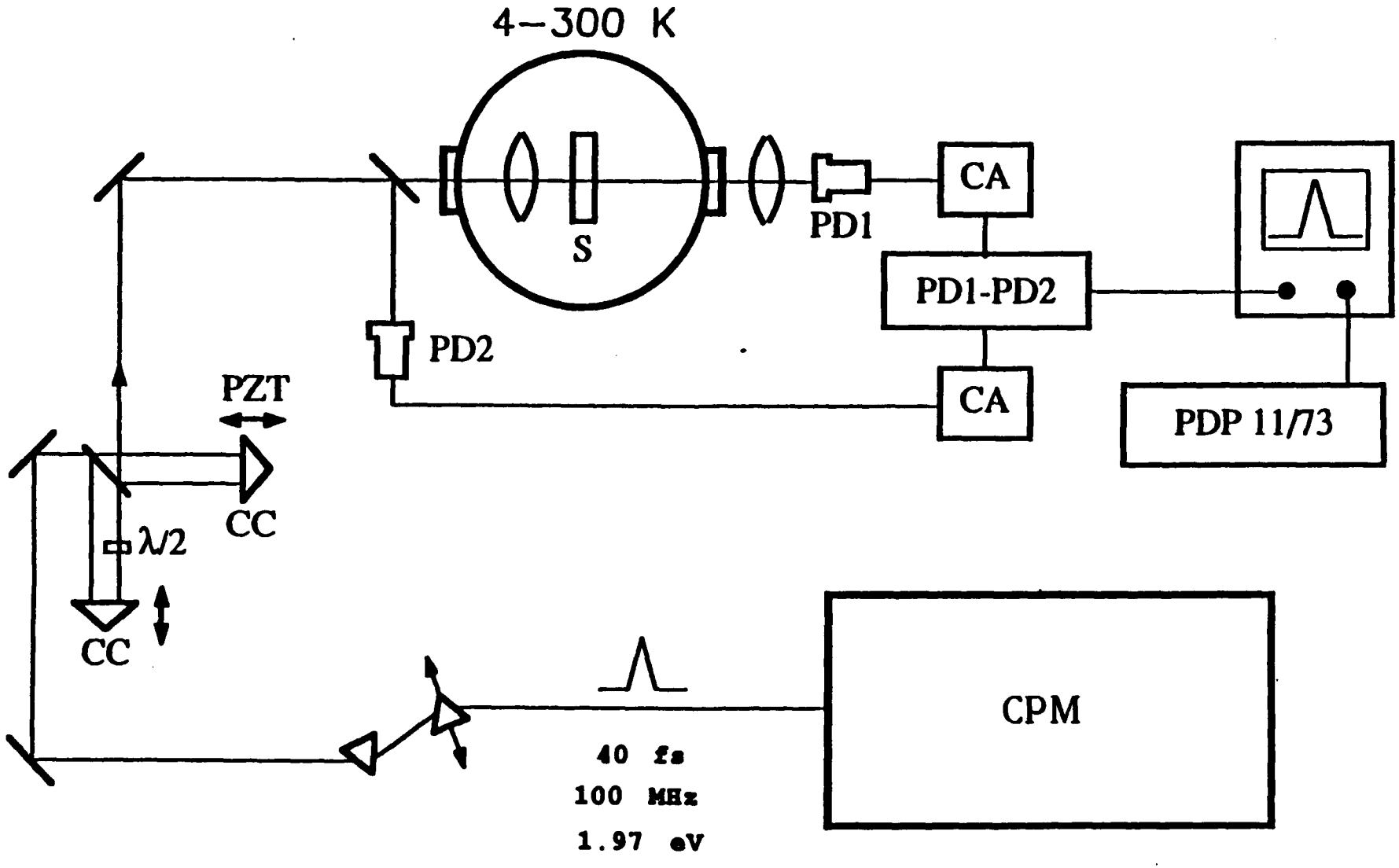
4–300 K
S
PD1
CA
PD1-PD2
PD2
CA
PZT
CC
λ/2
CC
CPM
40 fs
100 MHz
1.97 eV
PDP 11/73

Data processing; linear prediction least squares fitting

-autoregressive fitting of the time series

-solve linear least squares problem for the linear prediction coefficients

-SVD allows distinction between signal and noise components (Kumaresan and Tufts, 1983)

-reconstruct signal estimator from truncated linear prediction filter

$$\Delta T(\tau) = \sum a_i \exp(-t/\tau_i) \cos(\omega_i \tau + \phi_i)$$

This method has several important features;

-no initial guess about the number of components is required

-eliminates need for nonlinear least squares fitting

-higher resolution than FFT for short time series

All damped sinusoidal components that are present in the signal are found, without prior knowledge of the signal form and limited only by the SNR of the data.

Typical results; 50% C.A.

SNR = 60dB, 3 components, $\Delta(\tau_i)^2 = 10\%$

$\Delta(a_i)^2 = 20\%$

CENTER FOR OPTO-ELECTRONIC SYSTEMS RESEARCH

FEMTOSECOND RELAXATION PROCESSES IN SEMICONDUCTORS

Femtosecond Time-resolved Spectroscopy

Enhanced temporal resolution

Semiconductors:

Characterisation of high-speed electronic devices

Ballistic transistors

Velocity-overshoot devices

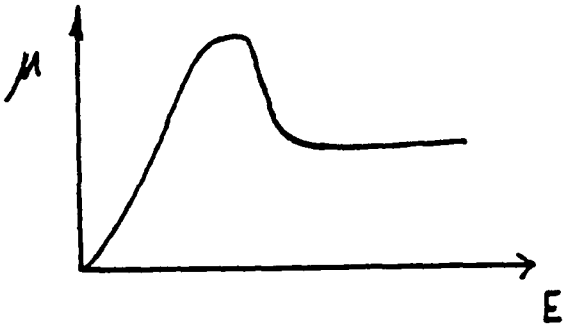

(GaAs).

Molecules:

Fundamental physics of chemical reactions

Laser-selective chemistry

Band Structure and Optically Coupled Region for Bulk GaAs

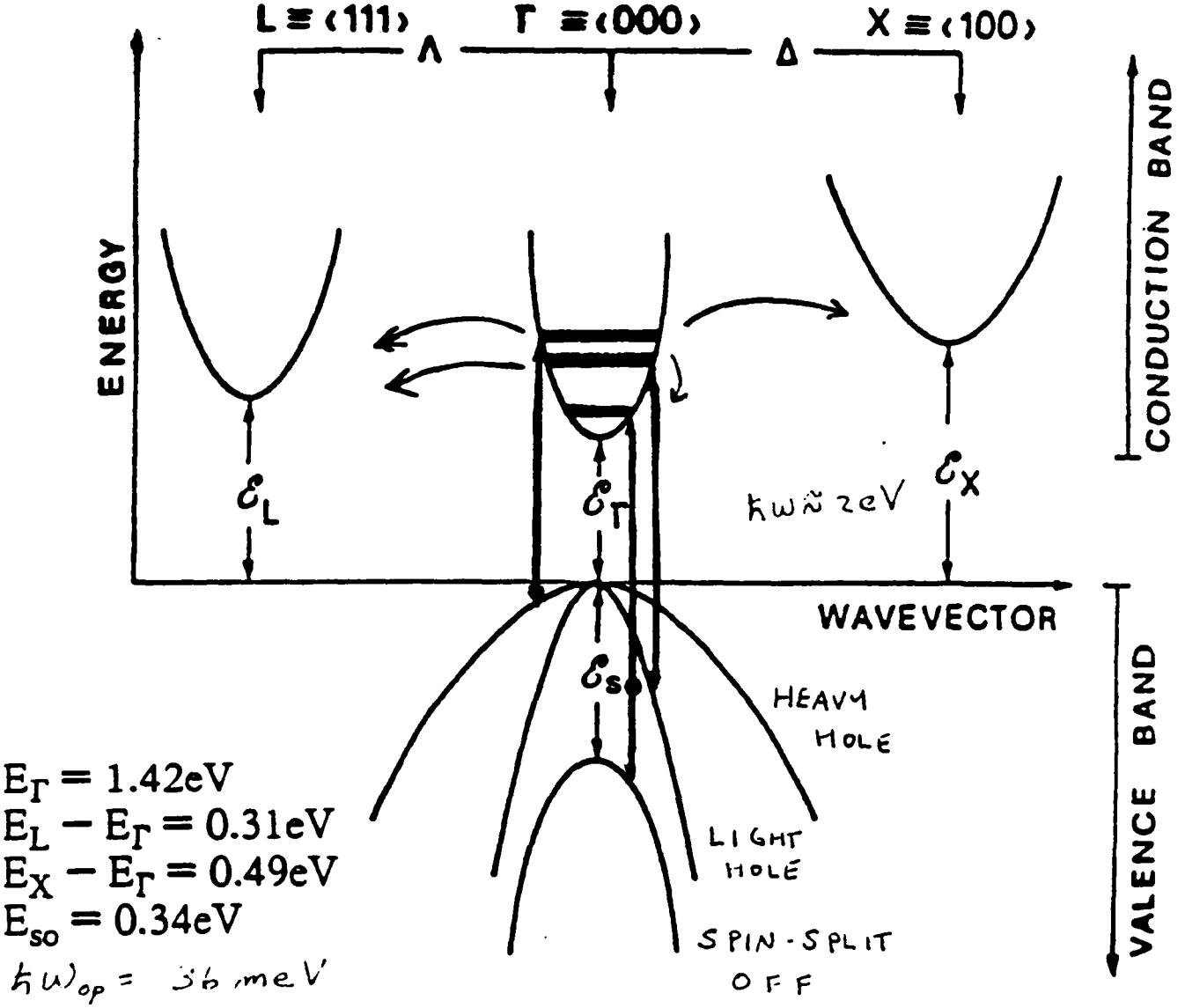

$E_\Gamma = 1.42eV$
$E_L - E_\Gamma = 0.31eV$
$E_X - E_\Gamma = 0.49eV$
$E_{so} = 0.34eV$
$\hbar\omega_{op} = 36\,meV$

- Three transitions from the valence bands into the Γ-valley conduction band are possible.

TRANSMISSION-CORRELATION PEAK (TCP) SIGNAL

SAMPLES AT 300K

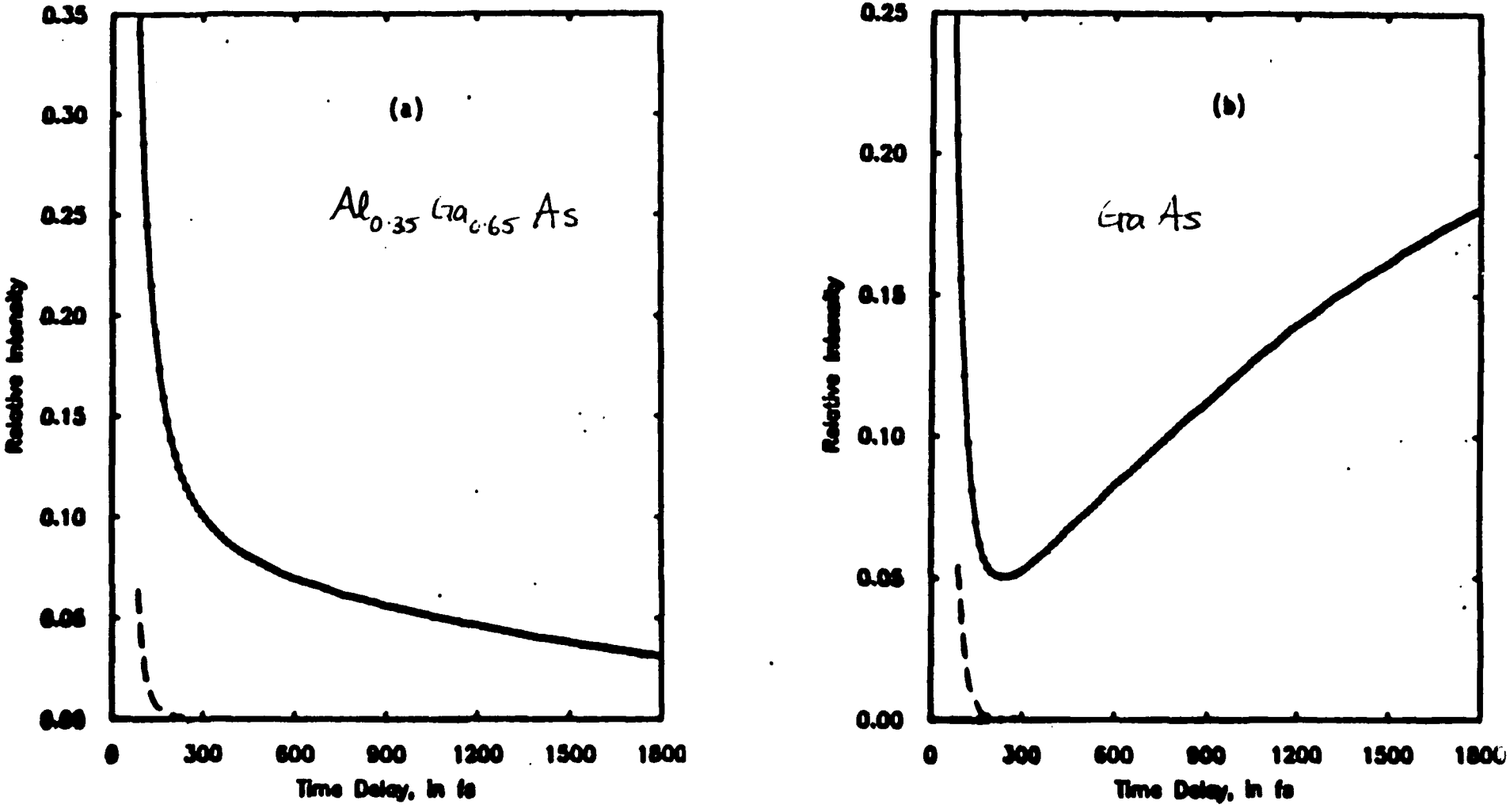

Fig.1

In both GaAs and $Al_{0.35}Ga_{0.65}As$, the subpicosecond decay is dominated by 2 exponential components.

$Al_{0.35}Ga_{0.65}As$

$T_1 = 40$ fs : Intervalley scattering by phonon emission and carrier- carrier scattering. (85%)

$T_2 = 140$fs : LO phonon emission. (9%)

+ long-lived component (1.6ps)

GaAs

$T_1 = 35$fs : IV + CC (85%)

$T_2 = 160$fs : LO (8%)

+ "rising wing" due to bandfilling

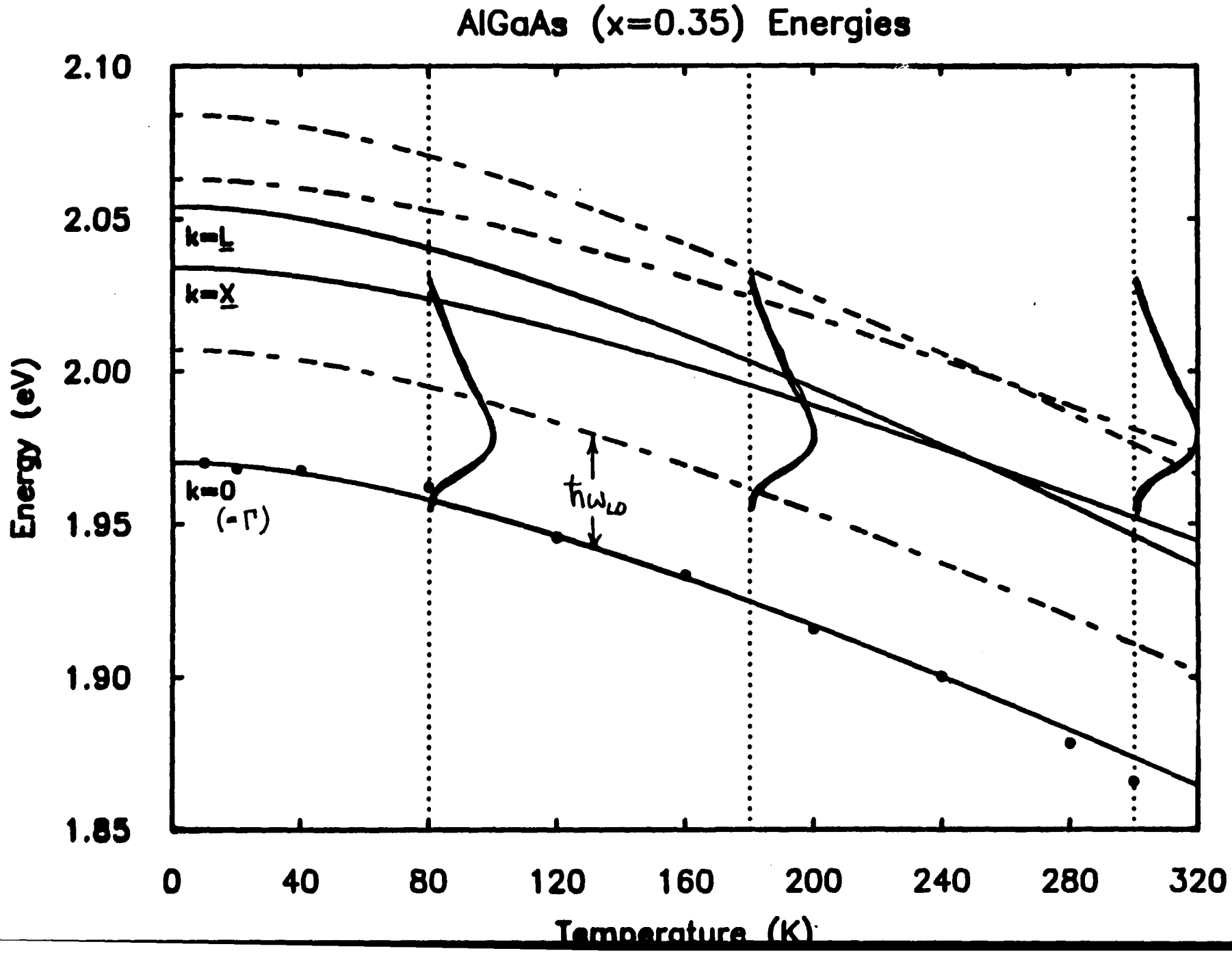
AlGaAs (x=0.35) Energies
2.10
2.05
2.00
1.95
1.90
1.85
Energy (eV)
k=L
k=X
k=0
(=Γ)
ħω_LO
0
40
80
120
160
200
240
280
320
Temperature (K)

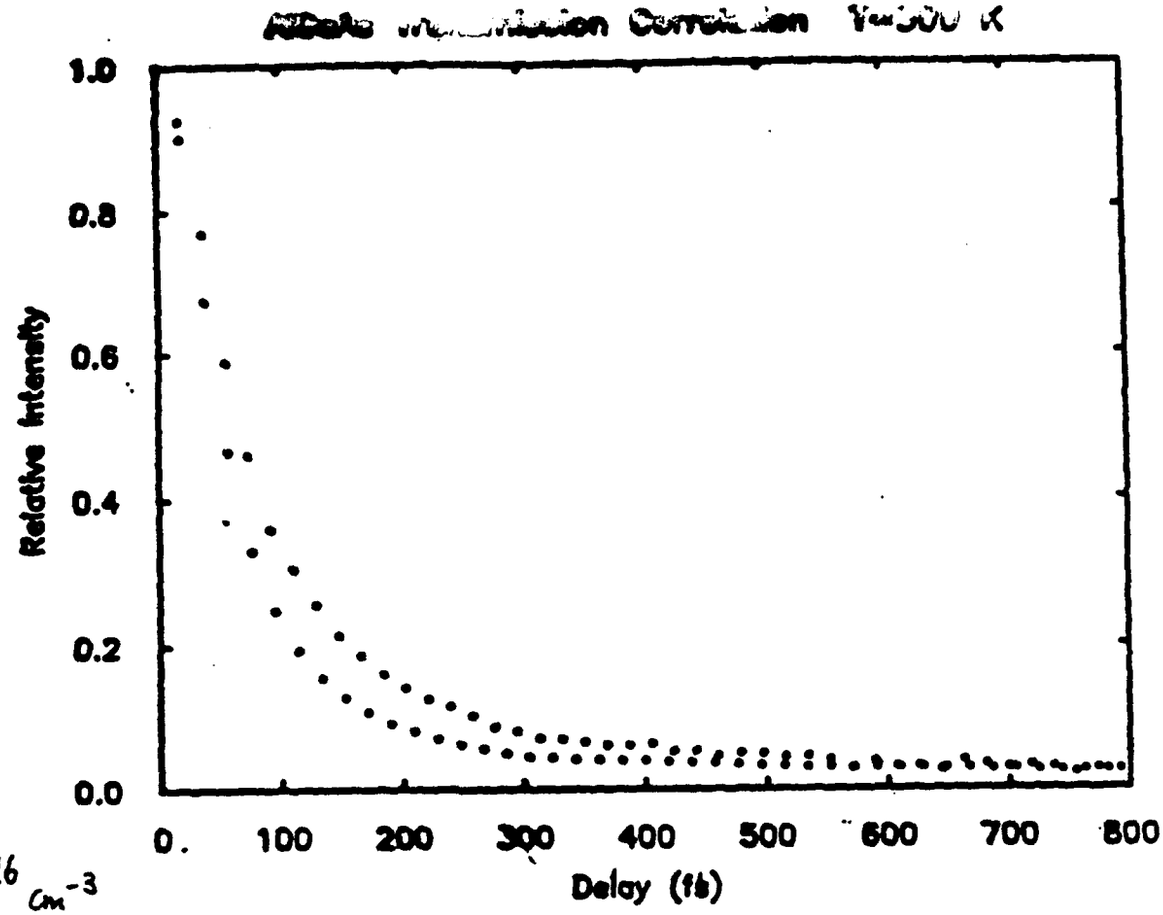

(a) 5×10^{16} cm^{-3}

(b) 3×10^{18} cm^{-3}

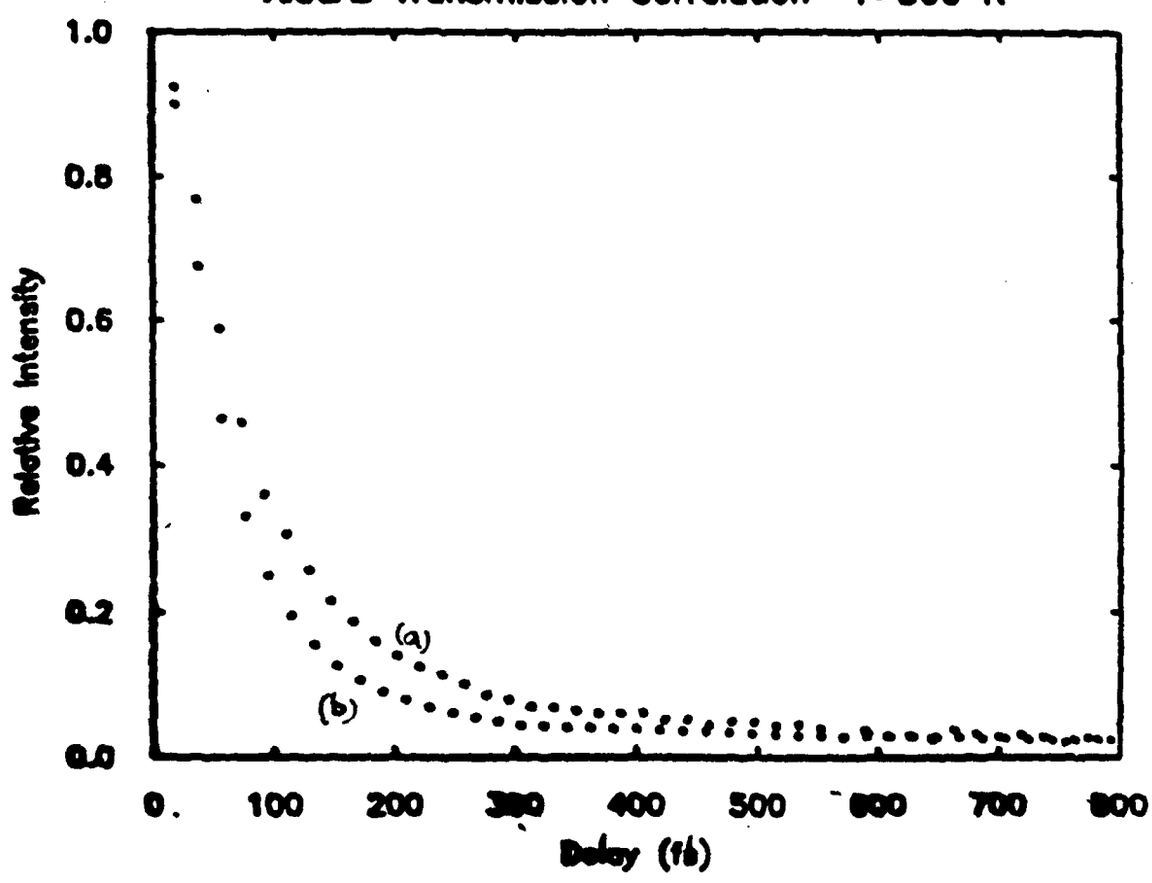

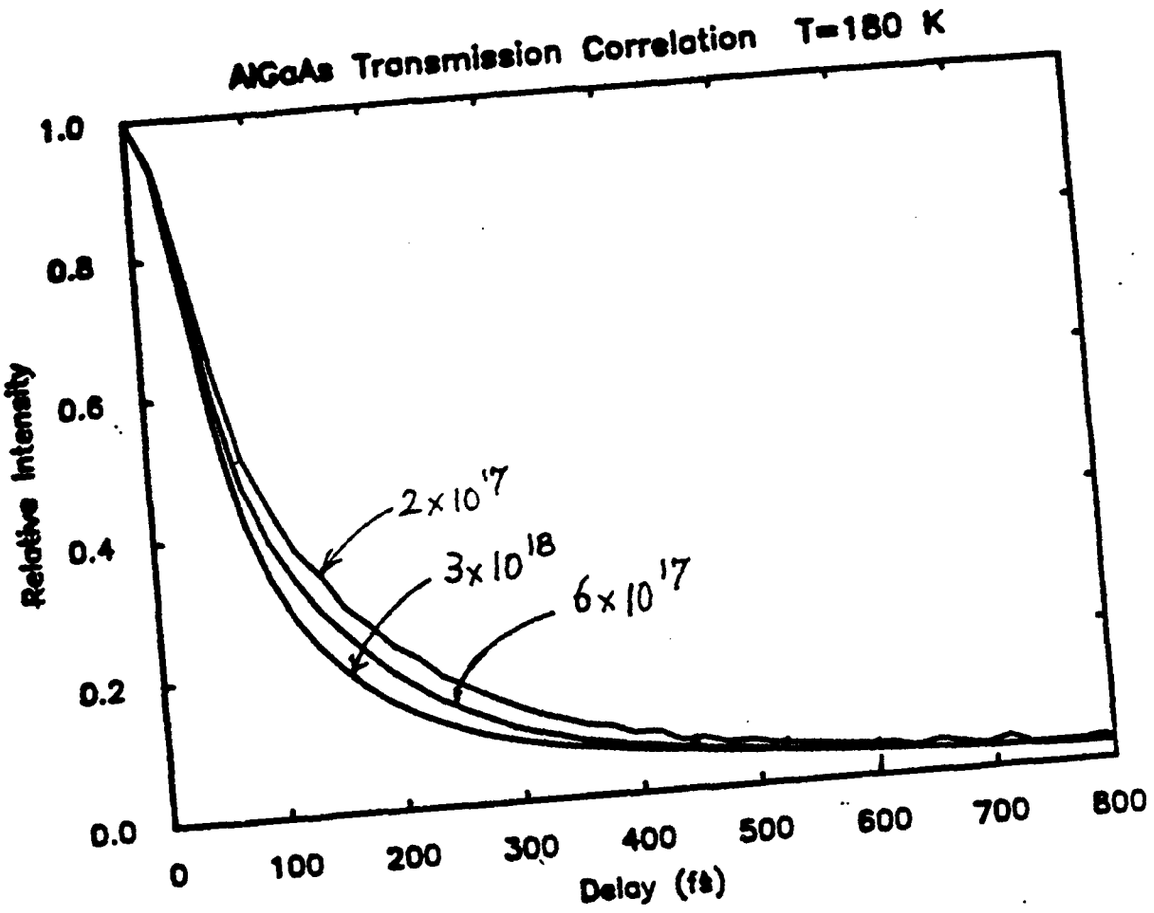
AlGaAs Transmission Correlation T=180 K
Relative Intensity
1.0
0.8
0.6
0.4
0.2
0.0
2x10^17
3x10^18
6x10^17
0
100
200
300
400
500
600
700
800
Delay (fs)

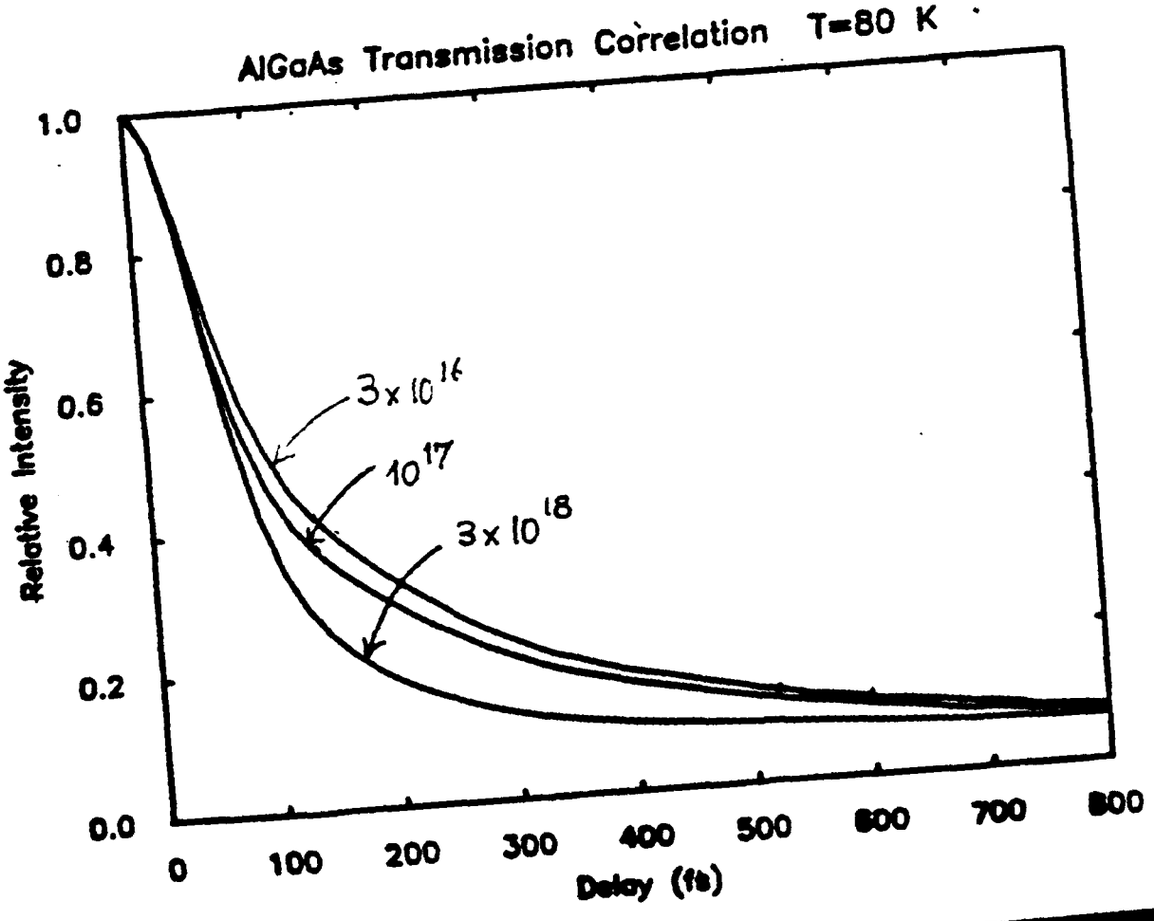
AlGaAs Transmission Correlation T=80 K
Relative Intensity
1.0
0.8
0.6
0.4
0.2
0.0
3x10^16
10^17
3x10^18
0
100
200
300
400
500
600
700
800
Delay (fs)

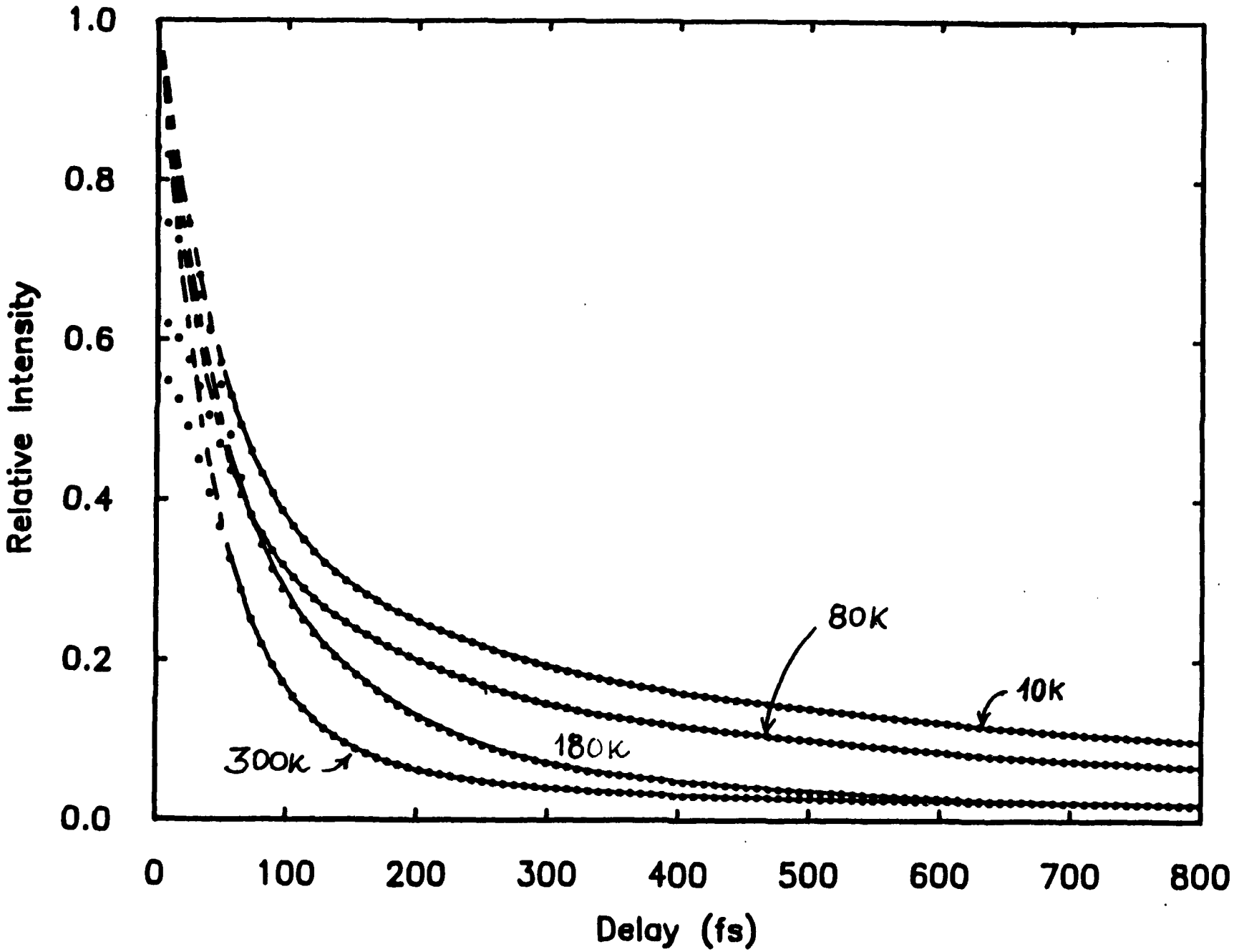
AlGaAs Transmission Correlation n=5x10^17 cm^-3
Relative Intensity
1.0
0.8
0.6
0.4
0.2
0.0
0
100
200
300
400
500
600
700
800
Delay (fs)
80K
10K
180K
300K

A 3 component exponential decay was found in all cases.

$n(t) = \Sigma\, a_i \exp(-t/\tau_i)$

$T_1 = 40$ fs : intervalley and carrier-carrier

$T_2 = 140$ fs : LO phonon emission

$T_3 = 1$ ps : (unspecified) depends on carrier density at 80K

For $n = 5 \times 10^{17}$ cm^{-3}

At	300K	$a_1/a_2 = 10$	
	180K	$a_1/a_2 = 3$	(IV disallowed)
	80K	$a_1/a_2 = 5$	(LO reduced)

Estimate of the efficiency with which each mechanism removes electrons from the initially excited states: from the measured TCP curves;

Delay	temp.	% of carriers removed	possible mechanisms
100fs	300K	84	IV+CC+LO
100fs	180K	75	CC+LO

-Then, roughly, of the carriers which leave the initial states in the first 100 fs

65% scatter to the satellite valleys

30% scatter via carrier-carrier interactions

5% scatter by LO phonon emission

Conclusions:

-The various physical mechanisms which govern the initial relaxation of photoexcited electrons in AlGaAs have been experimentally identified.

-Intervalley and carrier-carrier scattering occur on a 40fs timescale, and LO phonon emission on a 150 fs timescale.

-Intervalley scattering dominates the relaxation when it is energetically allowed.

Summary

-Resolved fastest electron scattering processes in AlGaAs;

implications for the ultimate speed of electron devices

-Observed THz quantum beats in organic dye molecules;

important in the determination of excited-state potential energy surfaces

-Possibilities for observing other coherent transient phenomena in semiconductors;

(coherent electric currents?)

Large organic dye molecules as a paradigm for semiconductors

-Energy scales and relaxation times are similar.

-Substantially fewer electronic states: easier to perform understandable experiments.

CENTER FOR OPTO-ELECTRONIC SYSTEMS RESEARCH
FEMTOSECOND SPECTROSCOPY OF LARGE MOLECULES

Femtosecond Spectroscopy of Large Molecules

I.A.Walmsley
The Institute of Optics
University of Rochester

F.W.Wise and C.L.Tang
Cornell University

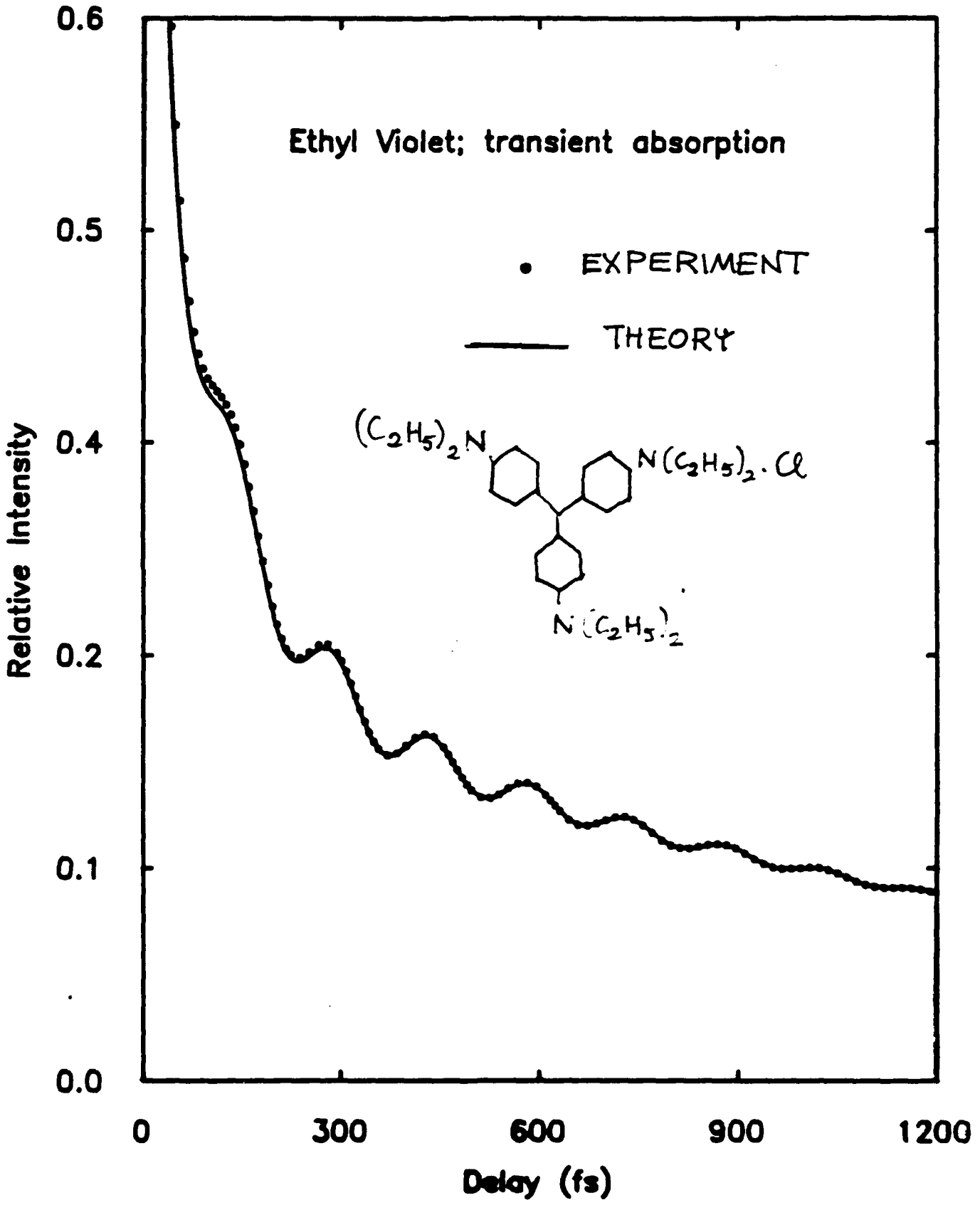
Ethyl Violet; transient absorption
EXPERIMENT
THEORY
$(C_2H_5)_2N$
$N(C_2H_5)_2 \cdot Cl$
$N(C_2H_5)_2$
Relative Intensity
0.6
0.5
0.4
0.2
0.1
0.0
0
300
600
900
1200
Delay (fs)

- QUANTUM BEATS:

  - MODULATION OF FLOURESCENCE, (ABSORPTION, BIREFRINGE etc) OF A SYSTEM EXCITED VIA SEVERAL INDISTINGUISABLE CHANNELS.

  - COHERENT SUPERPOSITION OF STATES DEVELOPING IN TIME.

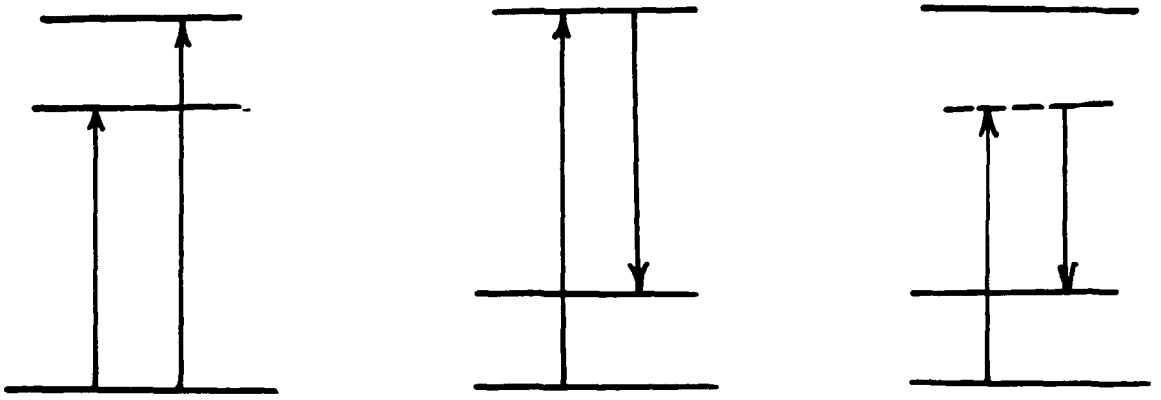

  - e.g. MOLECULAR SYSTEM:
    EXCITE A VIBRATIONAL MODE IN A GROUND- OR EXCITED-ELECTRONIC STATE.

-frequency of sinusoid same as Stokes shift of Raman-active mode

τ(measured) = 149fs; τ(expected) = 143fs

-does not depend on solvent viscosity

-impulsive excitation of molecular nuclear vibrational mode

$$\ddot{Q} + \Gamma \dot{Q} + \omega_0^2 Q = N (\delta\alpha/\delta Q) : E E$$

Q = vibrational amplitude
Γ = Raman linewidth
ω_0 = Raman frequency

-electric field must have spectrum as broad as ω_0

-pulses must be shorter than timescale of all dynamics

-time domain analog of Raman scattering

-molecular structure

tri-phenyl methane

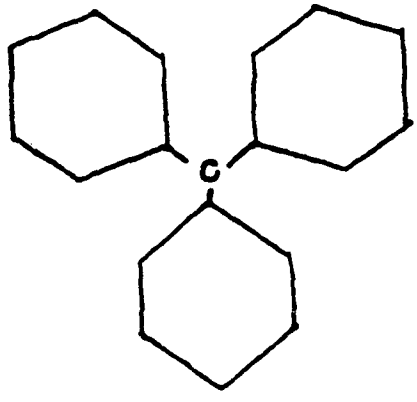

-schematic energy levels

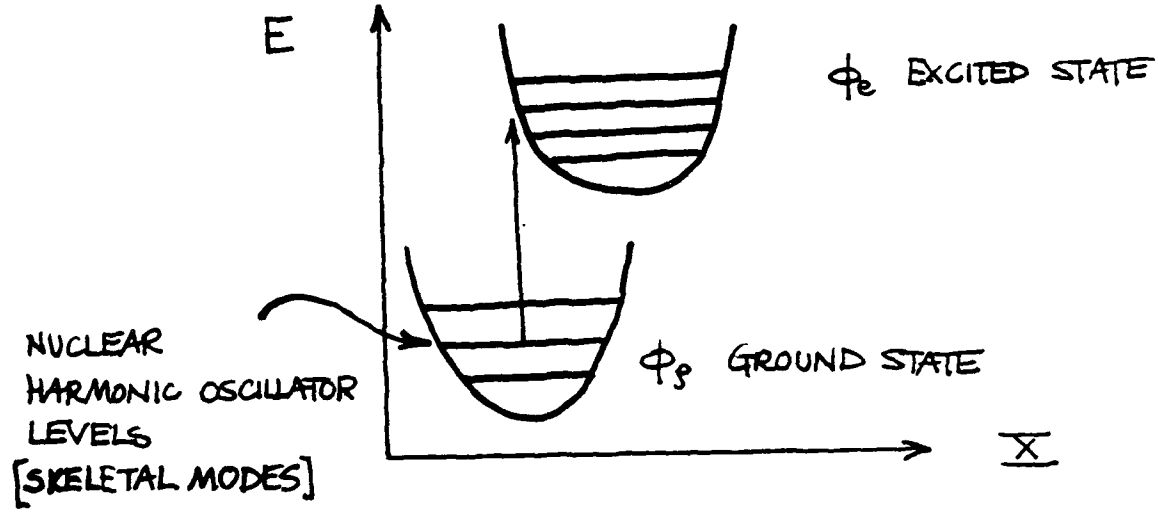

-only 3 levels are important in the interaction
(Raman selection rules)

TABLE -

$$y(t) = \sum a_i \exp(-t/T_i) \cos(2\pi\nu_i t + \phi_i)$$

Molecule	a	T (fs)	ν(THz)	φ(deg)
Malachite Green	0.58	75		
	0.36	4800		
	0.06	205	6.60	11
Ethyl Violet	0.60	120		
	0.33	1700		
	0.07	380	6.45	7
Methyl Violet	0.55	39		
	0.23	2650		
	0.19	150		
	0.03	280	6.40	7
Victoria Blue	0.57	30		
	0.31	10000		
	0.11	105		
	0.01	190	6.14	13
Methylene Blue	0.98	27		
	0.01	1470		
	0.002	380	7.7	2
DODCI	0.47	185	0.87	5
	0.32	1050		
	0.09	370	6.35	3
	0.07	300	2.61	9
	0.03	180	8.17	93
	0.02	500	5.00	8
Nile Blue	0.72	43		
	0.20	400		
	0.04	180	4.86	140
	0.02	490	3.06	87
	0.006	560	5.00	12
	0.005	405	8.39	144
	0.005	4300	2.16	21
	0.0007	4700	6.96	73
	0.0004	3900	9.12	93
	0.0003	11500	10.6	27

Theory

-3rd order perturbation solution to Liouville equation for 3-level system.

-signal form is relatively independent of dephasing and population lifetimes of optical transitions.

probing polarisibility, not polarisation

-useful in regimes where other time-domain techniques, such as photon echoes, are not possible.

-phase of sinusoids depend on nature of exciting pulses and particular energy level scheme

PROBE PULSE WIDTH DEPENDENCE OF TCP SIGNAL

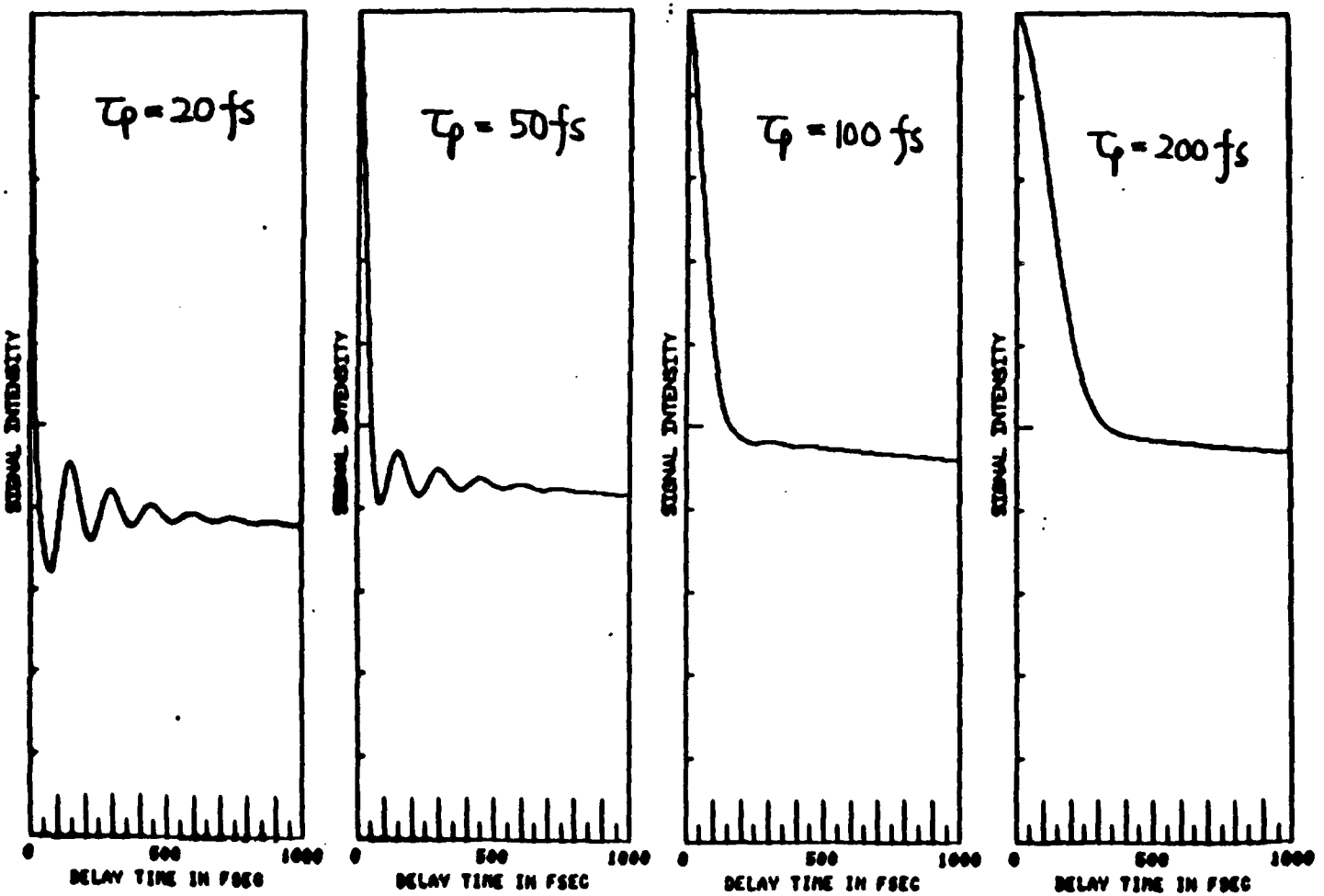

$T_1 = 4.8$ ps $\quad T_{2s} = 190$ fs $\quad T_2 = 0 \quad \nu_{2a}^{-1} = 150$ fs.

DEPHASING RATE DEPENDENCE OF TCP SIGNAL INTENSITY.

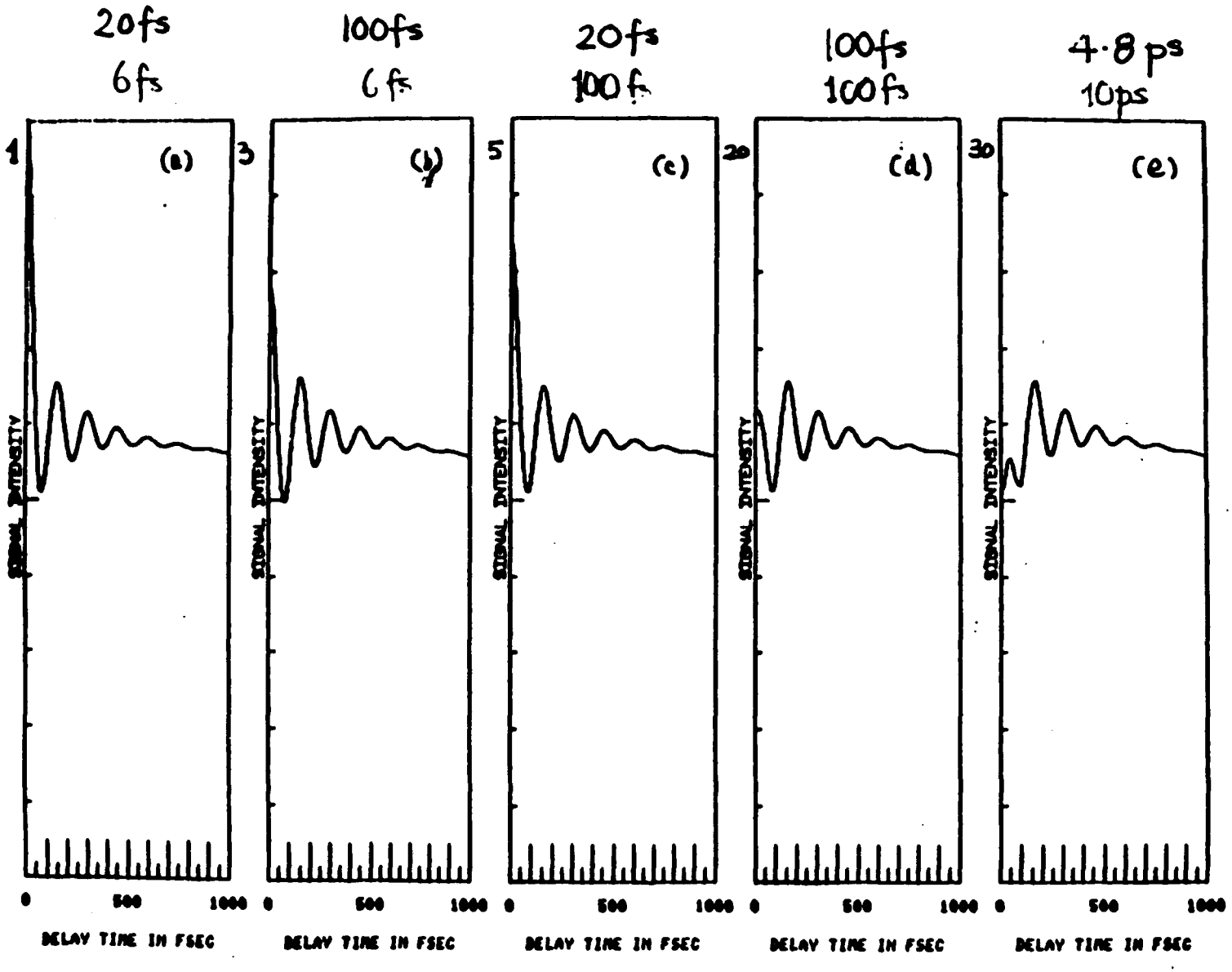

τ_p = 40fs T_1 = 4·8ps T_{2s} = 190fs ν_{22}^{-1} = 150 fs $|d_{31}|/|d_{21}| = 1$.

Measurements of the dephasing rates of optical transitions

- Phase of the quantum beats depends on the dipole moment decay rate $(T_2)^{-1}$

- Shape of signal is not very sensitive to T_2 or the inhomogeneous decay time.

-Phase of the beats depends on the phase of the phonon, which depends on the exact pulse shape, the population inversion etc.

-Solution . measure the phase of the beats through a spectrometer!

THREE - LEVEL MODEL.

EXCITATION

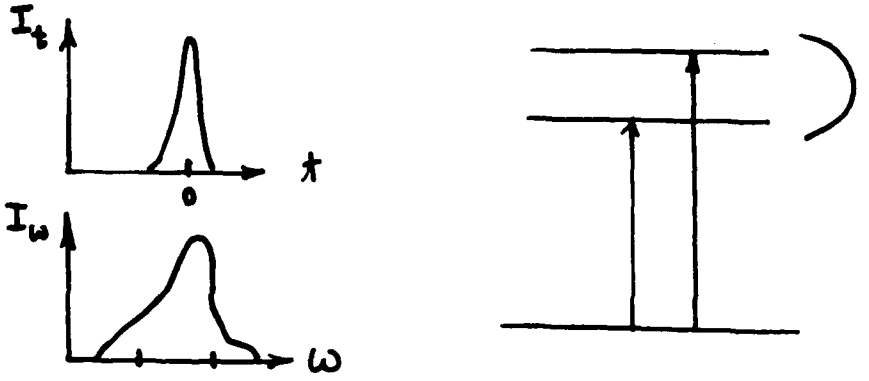

PRECESSION

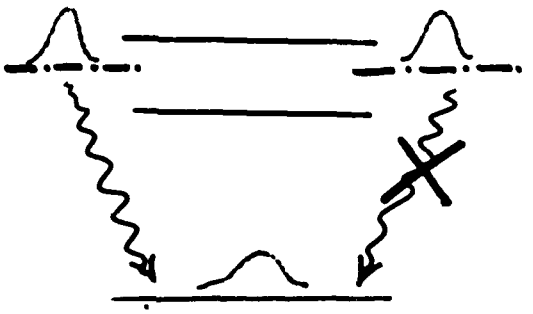

PROBE

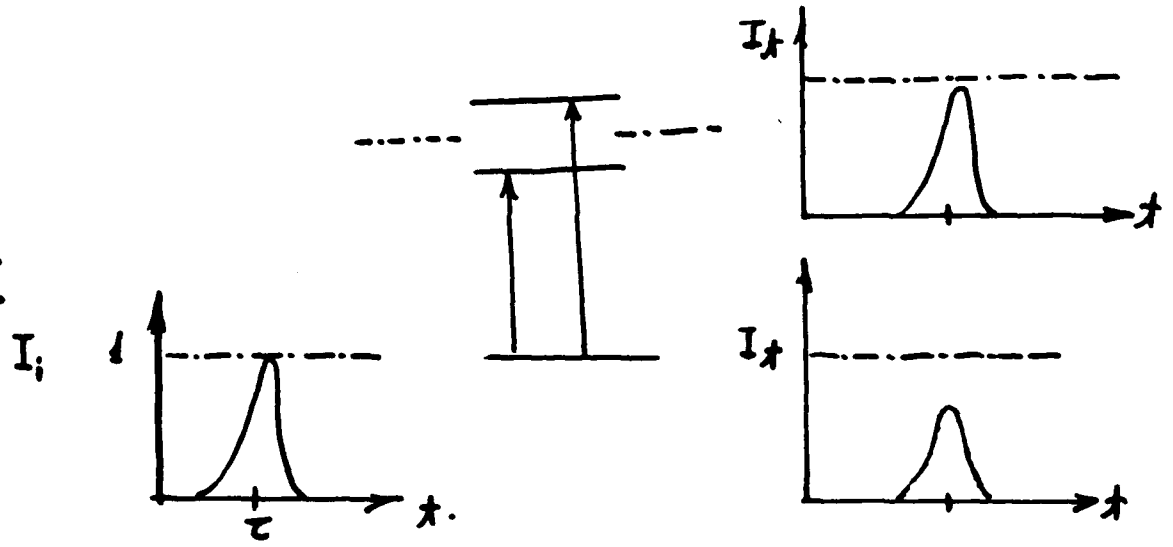

INCIDENT

TRANSMITTED.

-Spectrally-Resolved Absorption Saturation

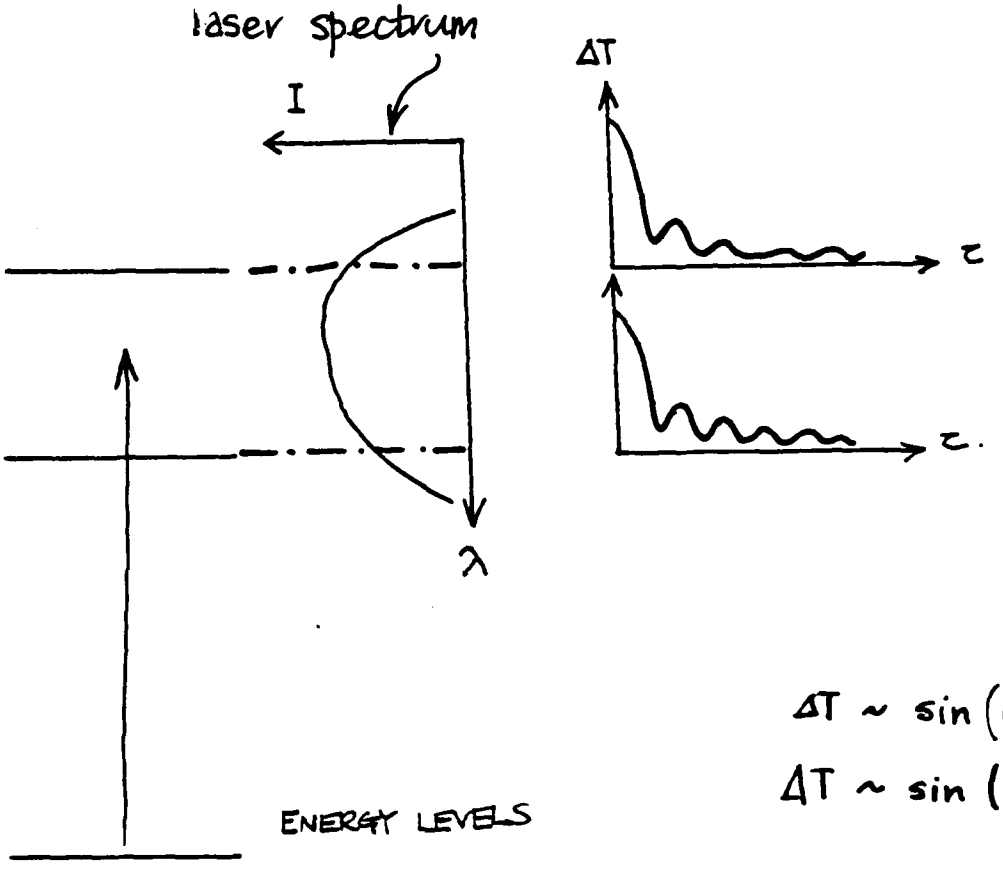

$$\Delta T \sim \sin(\omega t + \phi)$$

$$\Delta T \sim \sin(\omega t + \phi')$$

-phase of sinusoid is determined by ground- or excited-state sublevel excitation and pump detuning

- phase across spectrum depends only on g.s or e.s. sublevels.

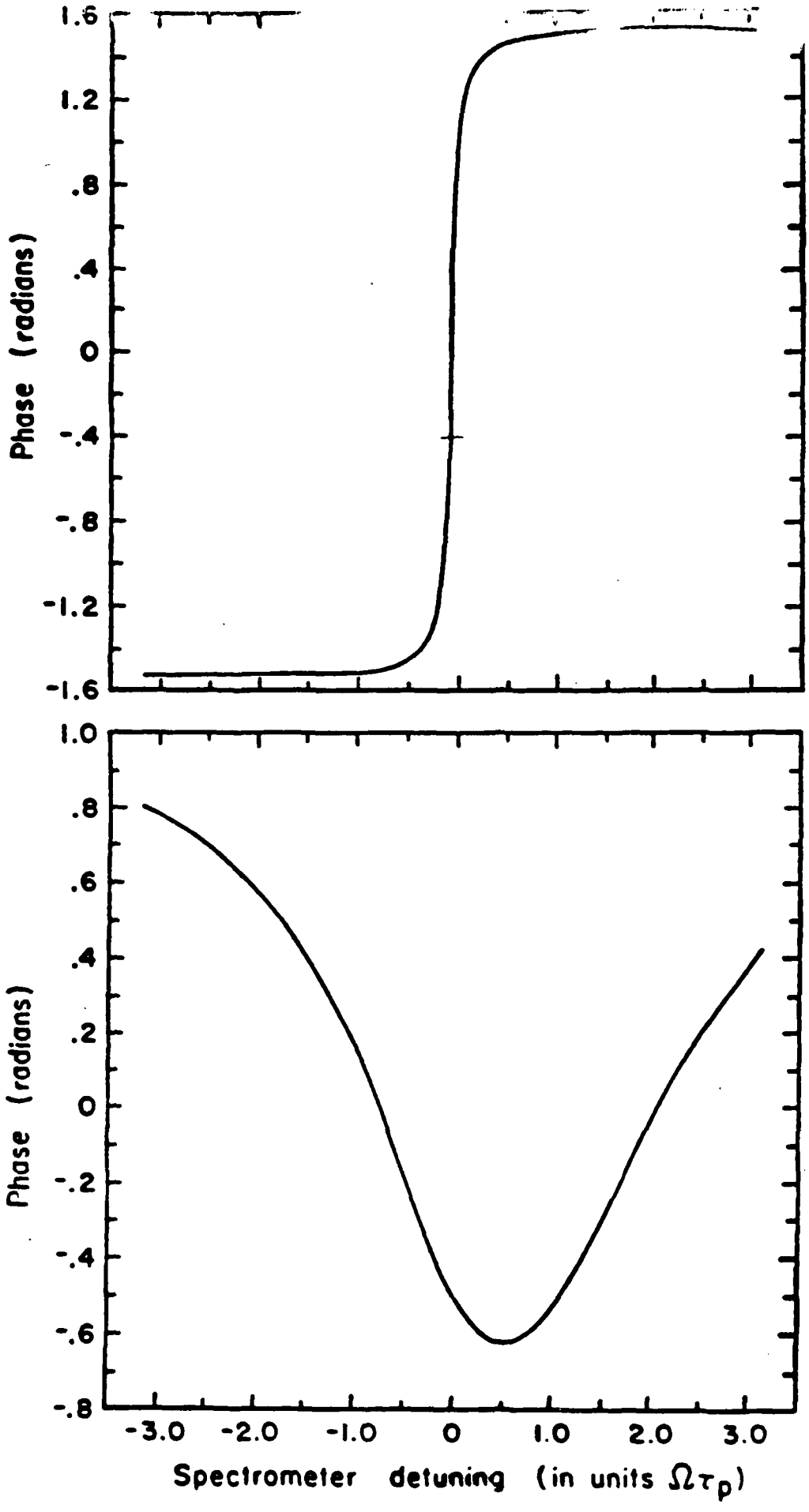
1.6
1.2
.8
.4
0
-.4
-.8
-1.2
-1.6
Phase (radians)
1.0
.8
.6
.4
.2
0
-.2
-.4
-.6
-.8
Phase (radians)
-3.0
-2.0
-1.0
0
1.0
2.0
3.0
Spectrometer detuning (in units $\Omega\tau_p$)

FROM: RUHMAN et al, J. CHEM. PHYS. 86, 6563, (1987).

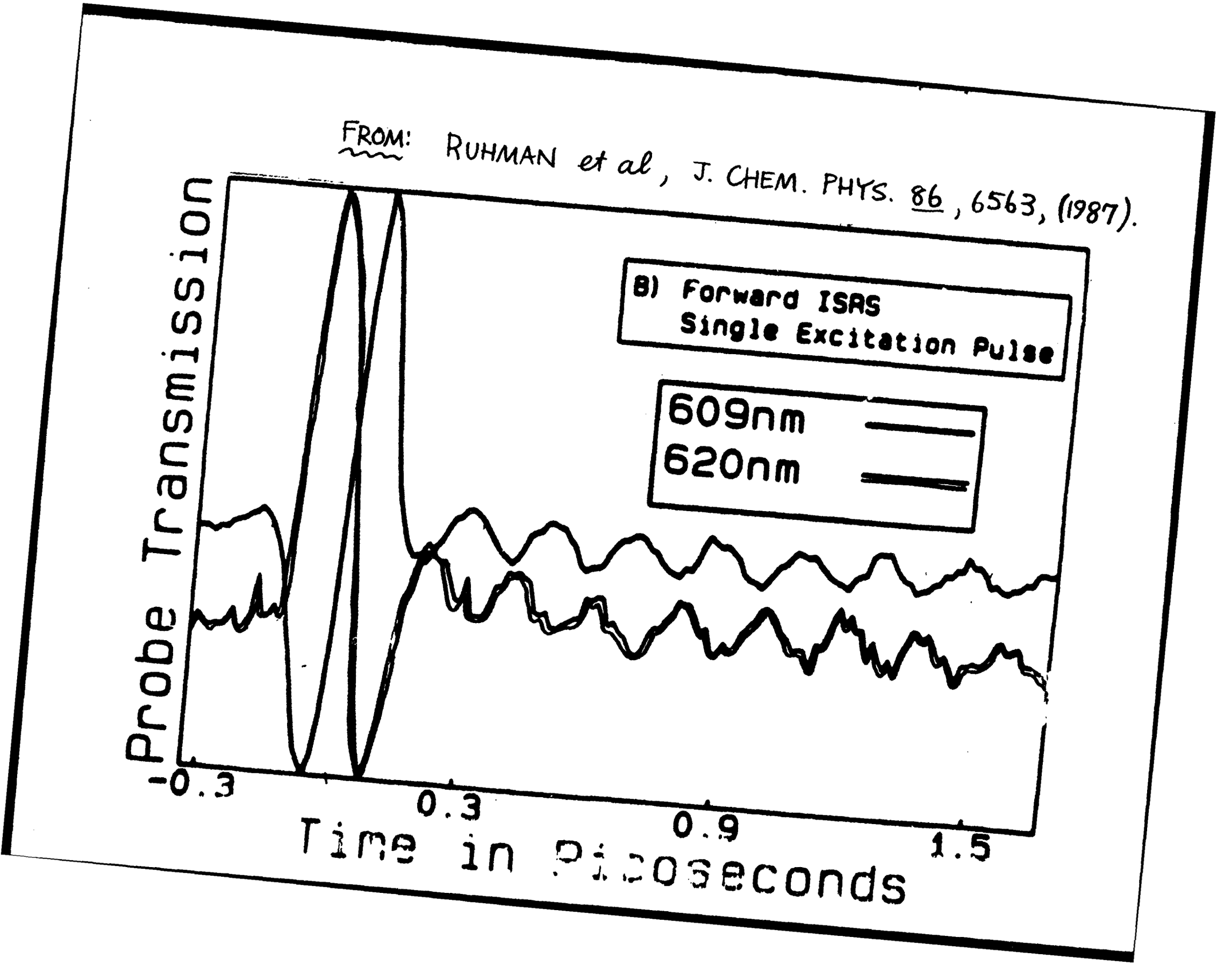

SPECTRALLY-RESOLVED TCP SIGNAL.

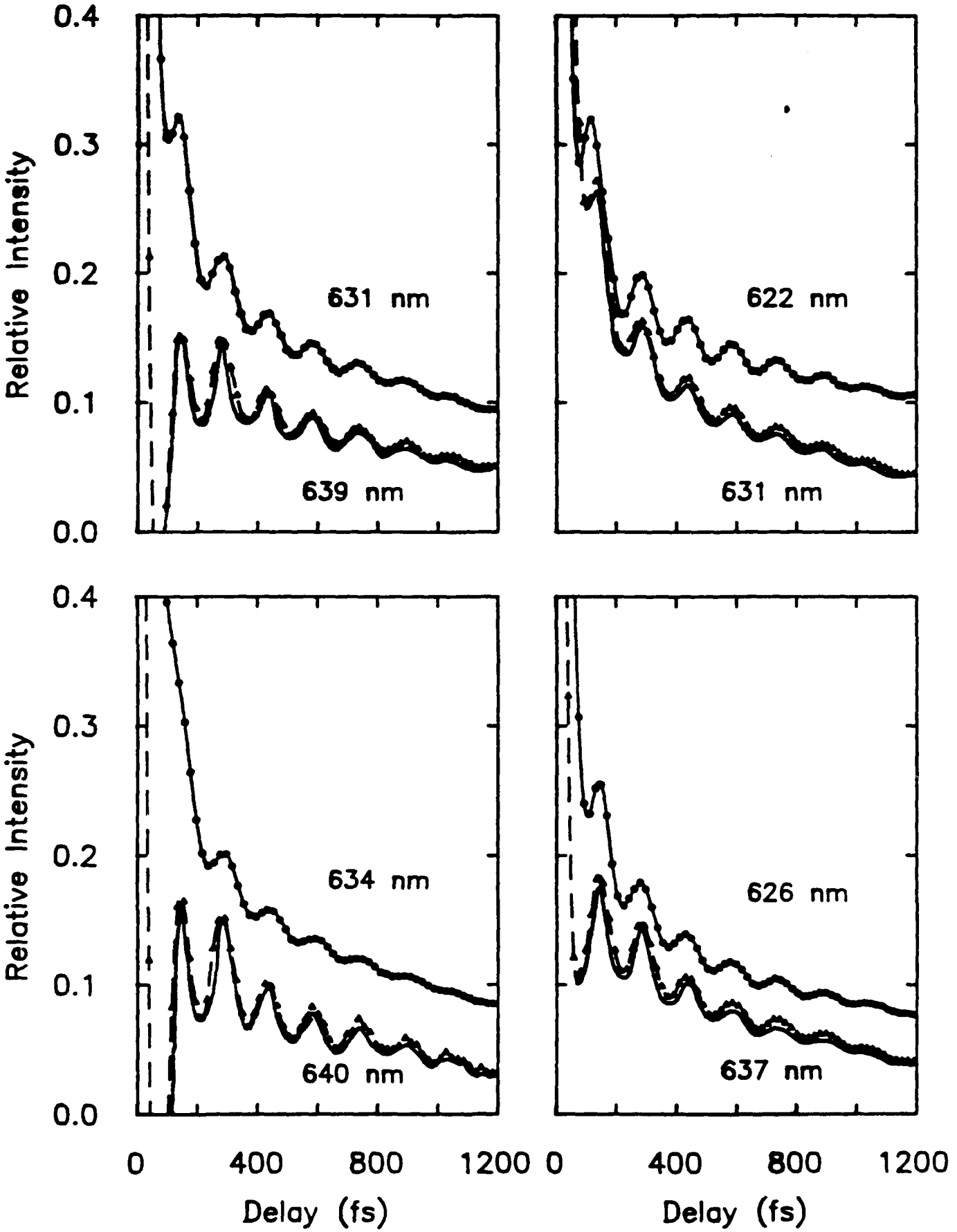

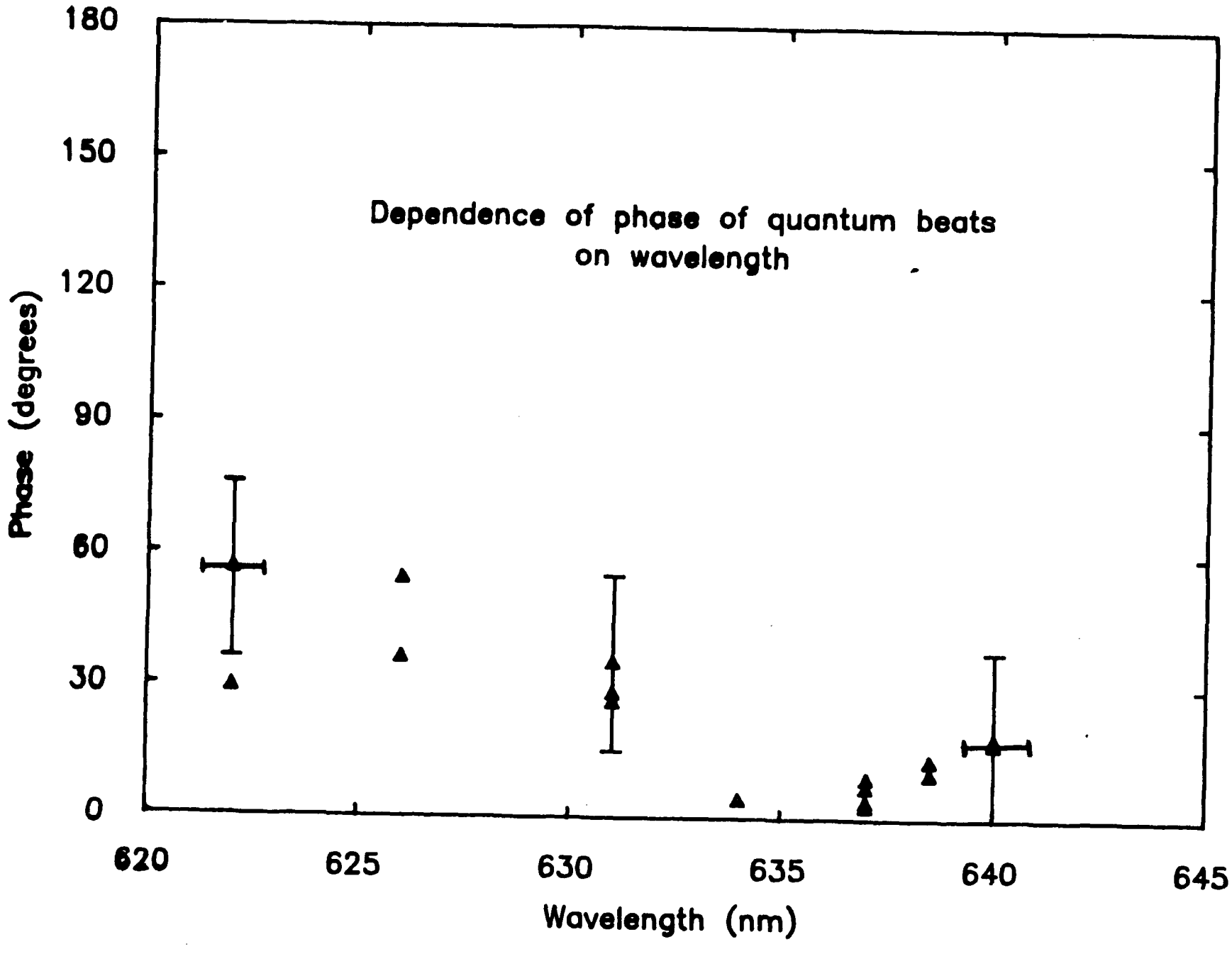
Dependence of phase of quantum beats
on wavelength
Phase (degrees)
180
150
120
90
60
30
0
620
625
630
635
640
645
Wavelength (nm)

EXPERIMENT: $T_2 \simeq 90-100$ fs

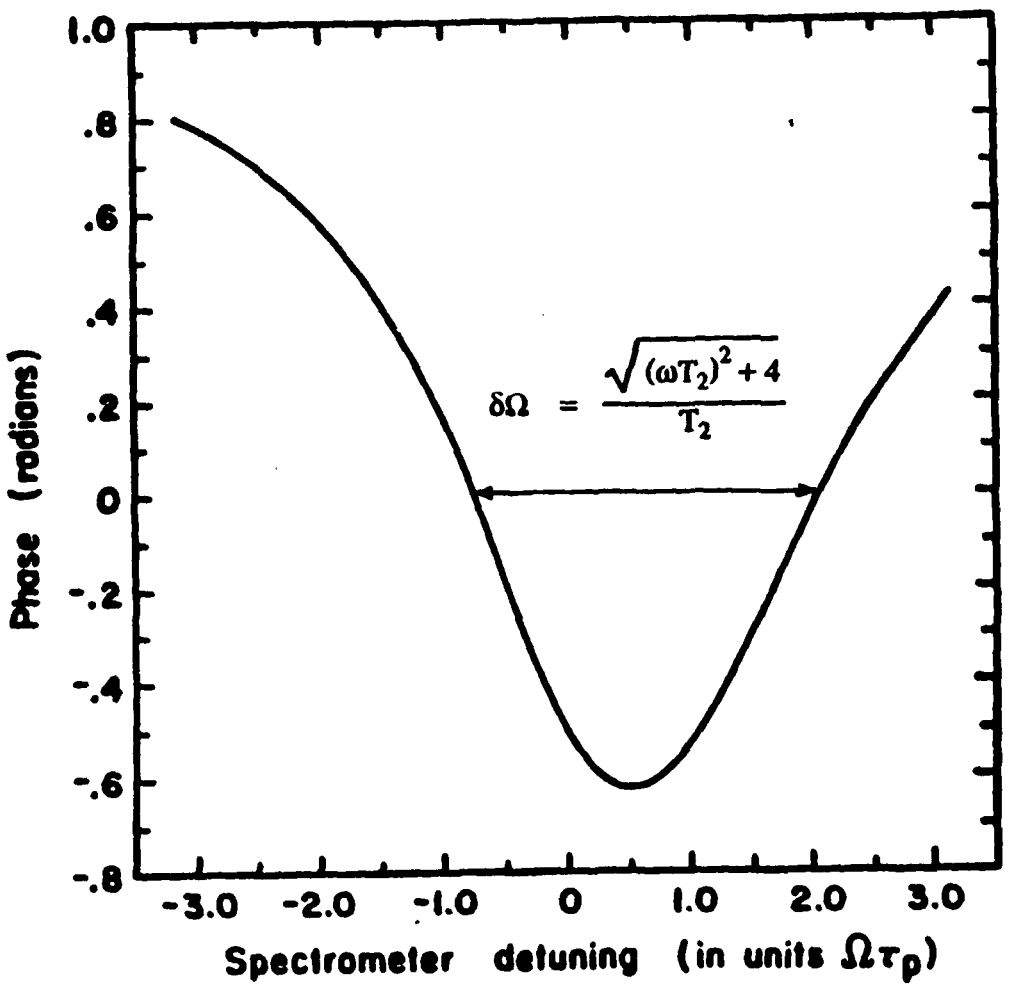

Fig.3 The phase of the modulations in the absorption signal as a function of spectrometer tuning (assuming the pump laser is on resonance). The FWHM of the curve is used to determine

Conclusions

-Observation of molecular nuclear motion in "real time" in organic dye molecules.

Implications for the determination of excited-state potential energy surfaces and laser-selective chemistry.

-Possible new method of measuring Raman linewidths.

Independent of the dephasing and population lifetimes of the optical levels.

-Technique for distinguishing ground- and excited-state quantum beats.

Important in understanding the dynamics of systems without prior knowledge of the energy level structure.

-Possibilities for observing other coherent transient phenomena in semiconductors.

{coherent optically-driven electric currents?}

Future Directions

- Relaxation on short timescales

For times short compared with the correlation time of the damping forces the decay of an elementary excitation (e.g. electronic states, phonons) is non-exponential.

An homogeneous line becomes inhomogeneous.

Use nonlinear optics to measure reservoir correlation functions

- Optical coherent transients in semiconductors

Excite electronic or phonon population impulsively and watch the wavepacket motion.

Time-domain observations of the phonon amplitude : measurements of anharmonic effects.

Time-domain observation of electron wavepacket motion : optical excitation of a phase-coherent electric current.

CENTER FOR NIGHT VISION AND ELECTRO-OPTICS

NONLINEAR OPTICS: MATERIALS RESEARCH

LASER RESEARCH TEAM: R & D of nonlinear optical materials, techniques, and concepts

- O Beam Control Devices
  - o Optical Switches
  - o Optical Isolators
  - o Filters
- O Laser Components
  - o New Sources
  - o Q-Switches
  - o Modulators

RECENT RESEARCH ACTIVITY:

- O Tungsten-Bronze Family of Ferroelectric Crystals (SBN & BSKNN)
  - o Ferroelectric Properties (Sensors)
  - o Electro-Optic Properties (Broad-Band Modulators)
  - o Photorefractive Properties
    - – *Optical Isolation of Coherent Beams Via Beam Fanning and Two-Beam Coupling*
    - – Phase Conjugation for Image Processing (Amplification, Storage, and Enhancement)
- O Nonlinear Organic Media (Short Pulse Studies)

NONLINEAR OPTICAL MATERIALS EFFORT

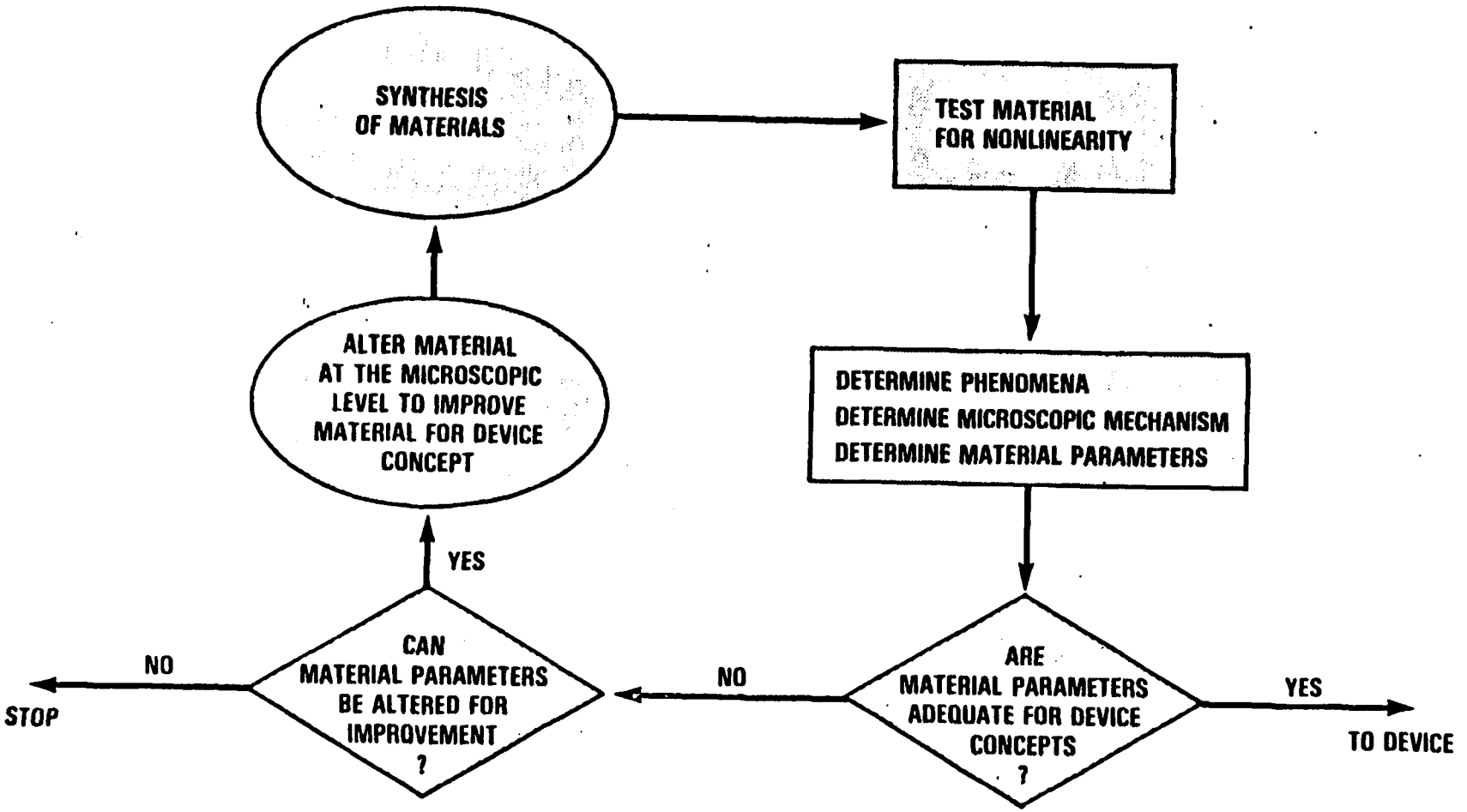

Nonlinear Phenomena (Self-Induced Effects)

Third-Harmonic Generation	THG	$\chi^{(3)}(-3\omega,\omega,\omega,\omega)$	$\frac{\lvert k_p \rvert}{\lvert k \rvert} = 3$
Nonlinear Refraction	NR(n_2)	$\chi^{(3)}_{Re}(-\omega,\omega,\omega,-\omega)$	$\bar{k}_p = \bar{k}$
Self-Focusing	SF	$\chi^{(3)}_{Re}(-\omega,\omega,\omega,-\omega)$	$\nabla^2_\perp A \neq 0$
Self-Defocusing	SD	$-\chi^{(3)}_{Re}(-\omega,\omega,\omega,-\omega)$	$\nabla^2_\perp A \neq 0$
Two-Photon Absorption	TPA	$\chi^{(3)}_{Im}(-\omega,\omega,\omega,-\omega)$	
Degenerate Four-Wave Mixing	DFWM	$\chi^{(3)}_{Re}(-\omega,\omega,\omega,-\omega)$	$\bar{k}_p \neq \bar{k}' = \bar{k}''$ $\lvert\bar{k}_p\rvert = \lvert\bar{k}'\rvert = \lvert\bar{k}''\rvert$
Stimulated Raman Scattering	SRS	$\chi^{(3)}_{Im}(-\omega_2,\omega_1,-\omega_1,\omega_2)$	
Stimulated Brillouin Scattering	SBS	$\chi^{(3)}_{Im}(-\omega_2,\omega_1,-\omega_1,\omega_2)$	$\omega_1 \sim \omega_2$
Raman-Induced Kerr Effect Scattering	RIKES	$\chi^{(3)}_{Re}(-\omega_2,\omega_1,-\omega_1,\omega_2)$	
Coherant Anti-Stokes Raman Scattering	CARS	$\chi^{(3)}_{Im}(-\omega_{AS},\omega_1,\omega_1,-\omega_2)$	

TABLE 1

NONLINEAR OPTICAL EFFECTS & APPLICATIONS

- EFFORT AT CNVEO TO DEVELOP A FUNDAMENTAL UNDERSTANDING OF NONLINEAR OPTICAL EFFECTS IN APPROPRIATE SPECTRAL RANGES

- EFFECTS STUDIED:
  - MULTIPHOTON ABSORPTION
  - SATURATION EFFECTS
  - SELF-FOCUSING/DEFOCUSING
  - STIMULATED SCATTERING
  - LASER INDUCED PLASMA ABSORPTION
  - PHOTOREFRACTION

- APPLICATIONS:
  - FAST OPTICAL SWITCHES & GATES
  - SECOND & THIRD HARMONIC GENERATION
  - FOUR WAVE MIXING (NEW SOURCES)
  - STIMULATED SCATTERING (NEW COHERENT SOURCES , PHASE CONJUGATION)
  - OPTICALLY BISTABLE DEVICES (LOGIC, FILTERING)
  - SATURABLE ABSORPTION (Q-SWITCHES, MODE-LOCKERS)
  - OPTICAL ISOLATORS/POWER LIMITERS
  - WAVE-FRONT REVERSAL, PHASE CONJUGATION

NONLINEAR MATERIALS

- O VIS-NIR
  - O LIQUID CRYSTALS
  - O ORGANIC SOLVENTS
  - O POLYMERS
  - O TUNGSTEN-BRONZE CRYSTALS
- O 3-5 MICRONS
  - O LIQIUD CRYSTALS
  - O TUNGSTEN-BRONZE CRYSTALS
  - O POLYMERS
- O 8-12 MICRONS
  - O CHALCOPYRITES
  - O LIQUID CRYSTALS
  - O ARTIFICIAL DIELECTRICS
  - O ARTIFICIAL KERR MEDIA
  - O METAL-SEMICONDUCTOR PHASE TRANSITION MATERIALS
  - O MULTIPLE QUANTUM WELLS SEMICONDUCTORS

KEY ISSUES

- TIME RESPONSE
- SENSITIVITY
- BANDWIDTH
- MATERIAL AVAILABILITY/QUALITY
- MATERIAL IMPROVEMENTS
- POSSIBILITY FOR NEW DEVICES

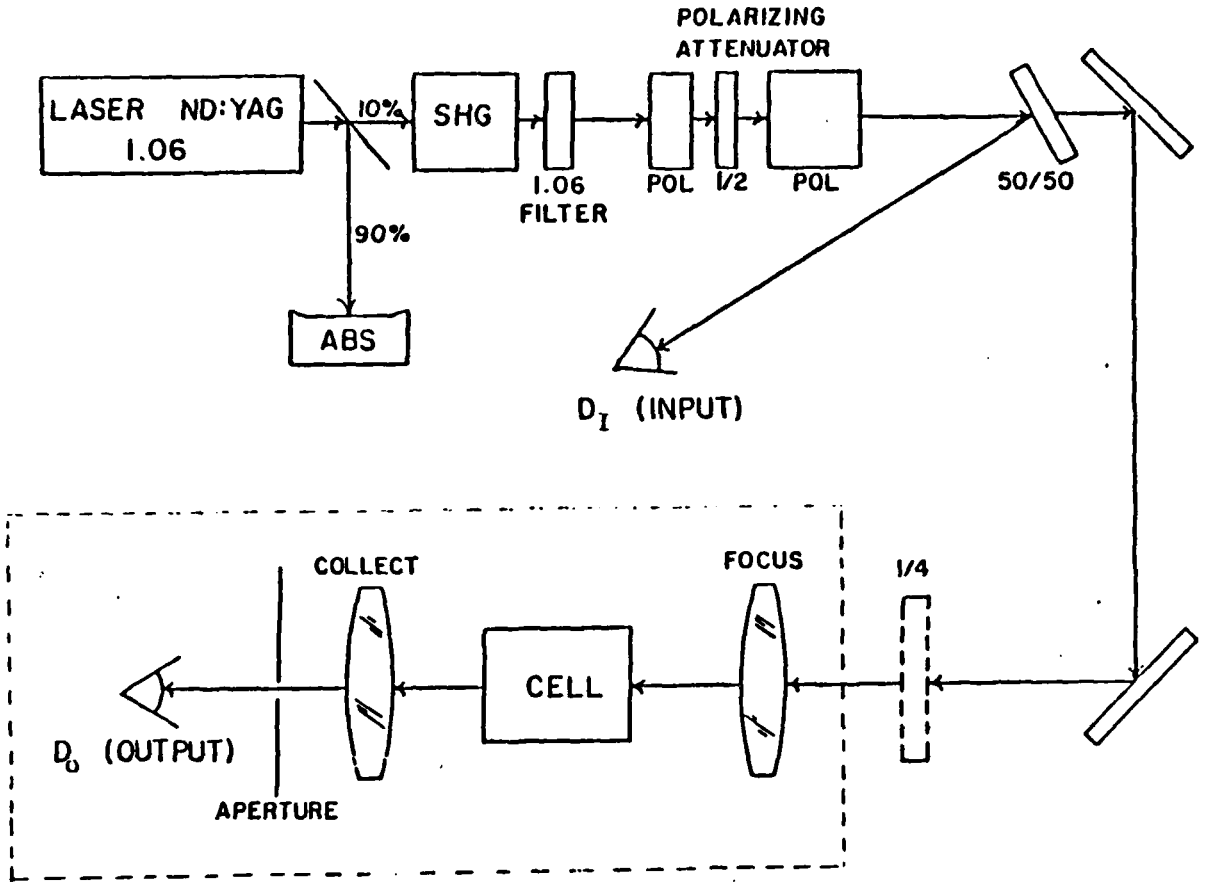
POLARIZING
ATTENUATOR
LASER ND:YAG
1.06
10%
SHG
1.06
FILTER
POL
1/2
POL
50/50
90%
ABS
D_I (INPUT)
COLLECT
FOCUS
1/4
CELL
D_o (OUTPUT)
APERTURE

FIGURE 2

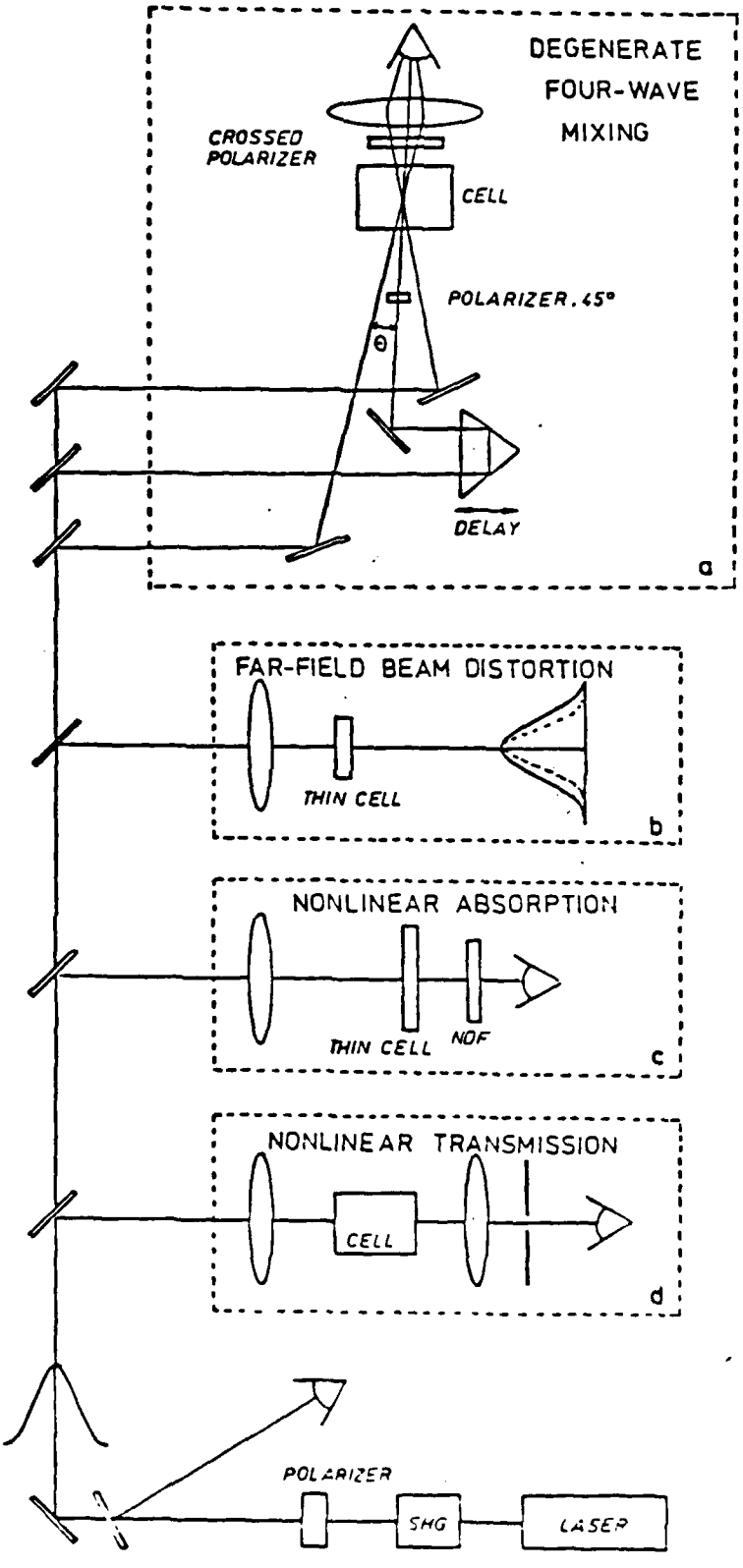
DEGENERATE
FOUR-WAVE
MIXING
CROSSED
POLARIZER
CELL
POLARIZER, 45°
θ
DELAY
a
FAR-FIELD BEAM DISTORTION
THIN CELL
b
NONLINEAR ABSORPTION
THIN CELL
NDF
c
NONLINEAR TRANSMISSION
CELL
d
POLARIZER
SHG
LASER

NONLINEAR TRANSMISSION

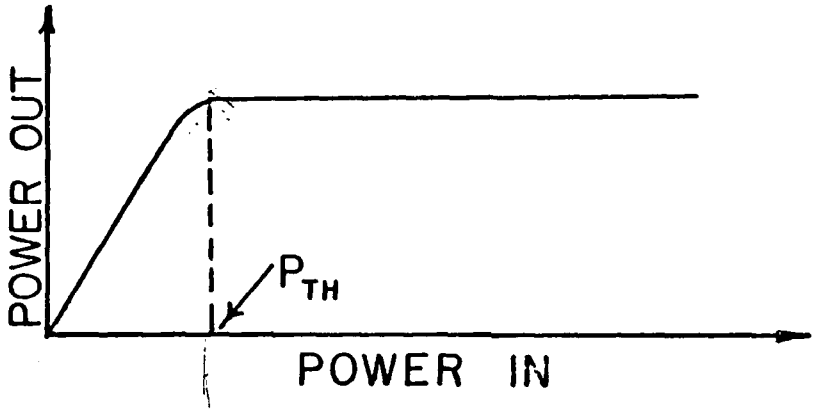

- THE THRESHOLD POWER P_{TH} CAN BE INFLUENCED BY A NUMBER OF NONLINEAR EFFECTS
  - ABSORPTION (LINEAR AND NONLINEAR)
  - SATURATION EFFECTS
  - SELF-FOCUSING/DEFOCUSING
  - SCATTERING
  - LASER INDUCED BREAKDOWN
- THE STRENGTH OF THE NONLINEARITY IS DETERMINED BY THE NONLINEAR INDEX COEFFICIENT n_2

$$n = n_o + n_2 \frac{|E_o|^2}{2}$$

NONLINEAR REFRACTION & ABSORPTION

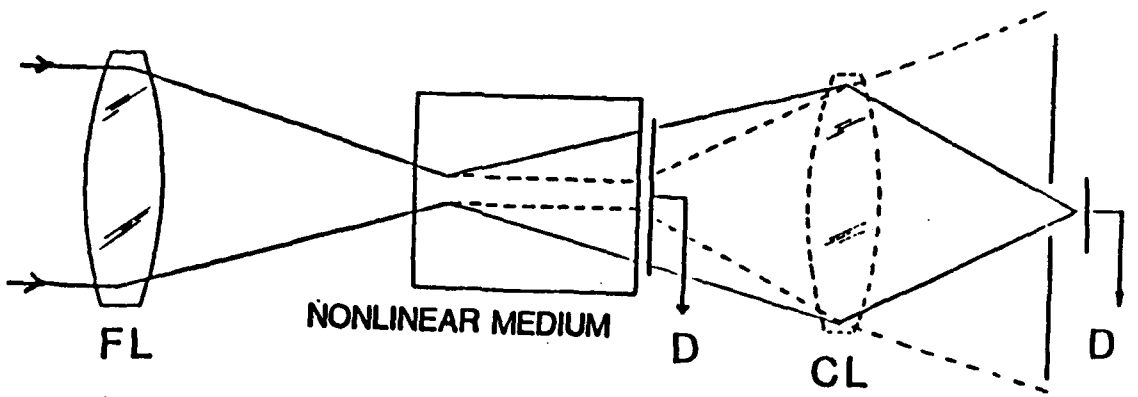

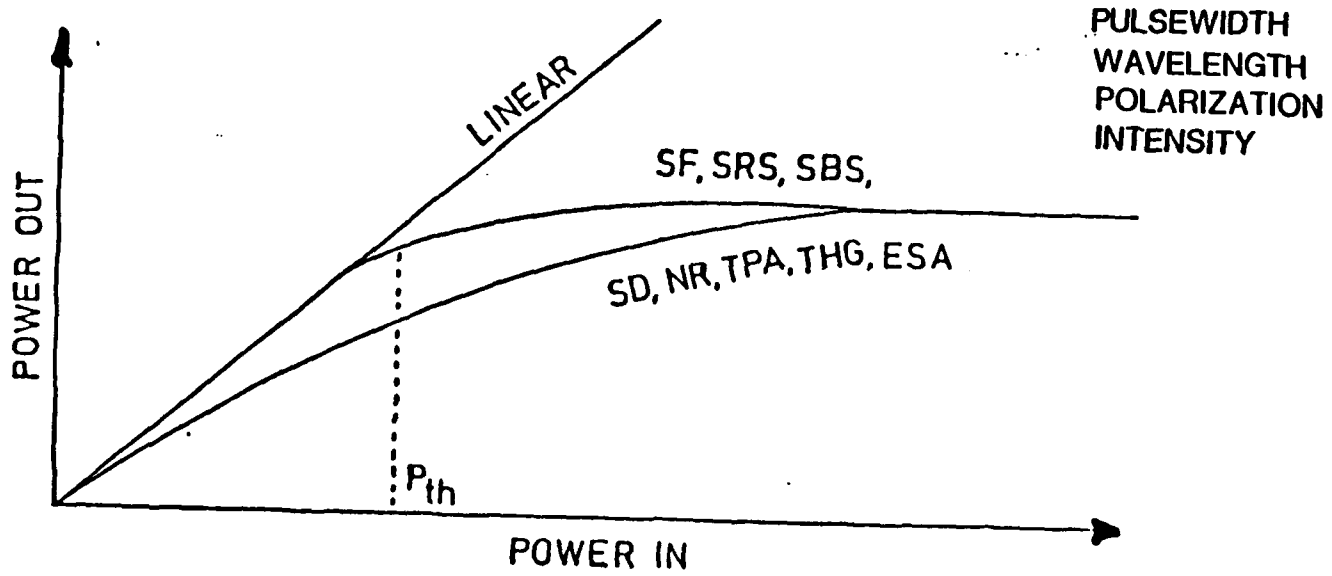

Linear Molecules

$S=C=S$

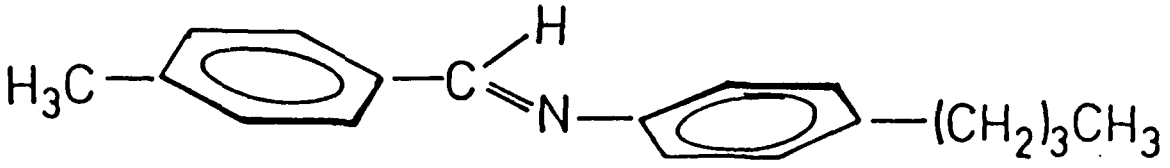

MEBBA

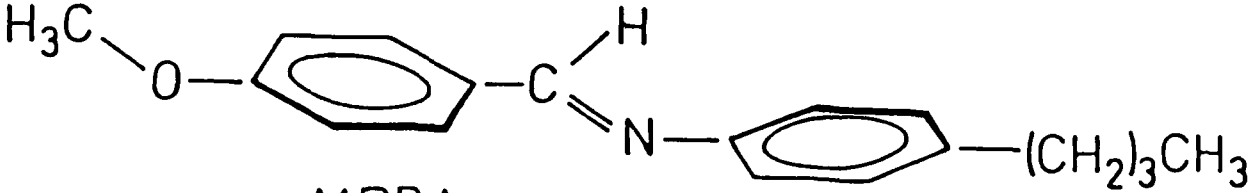

MBBA

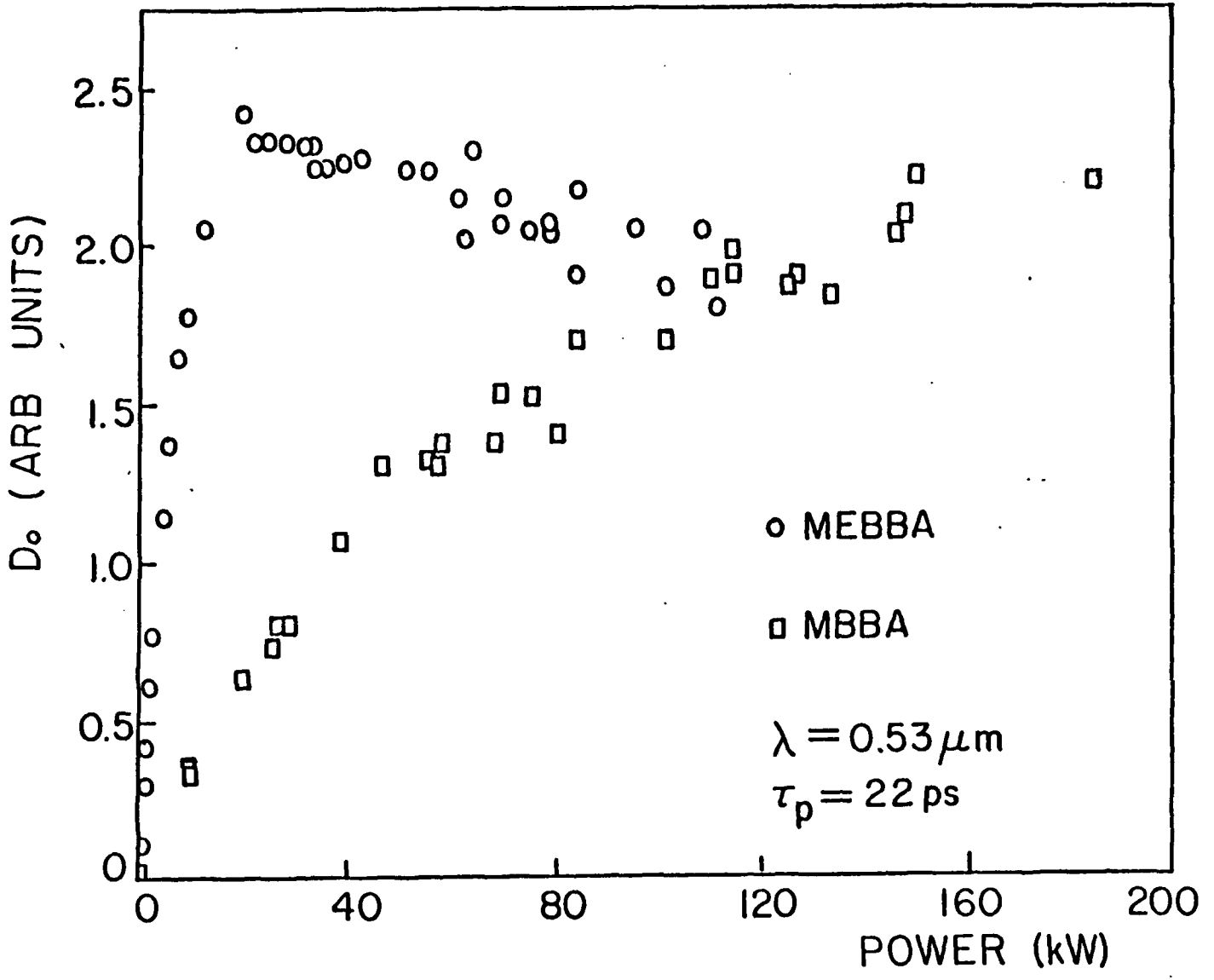
2.5
2.0
1.5
1.0
0.5
0
D_o (ARB UNITS)
0
40
80
120
160
200
POWER (kW)
o MEBBA
□ MBBA
$\lambda = 0.53\,\mu m$
$\tau_p = 22\,ps$

FIGURE 6

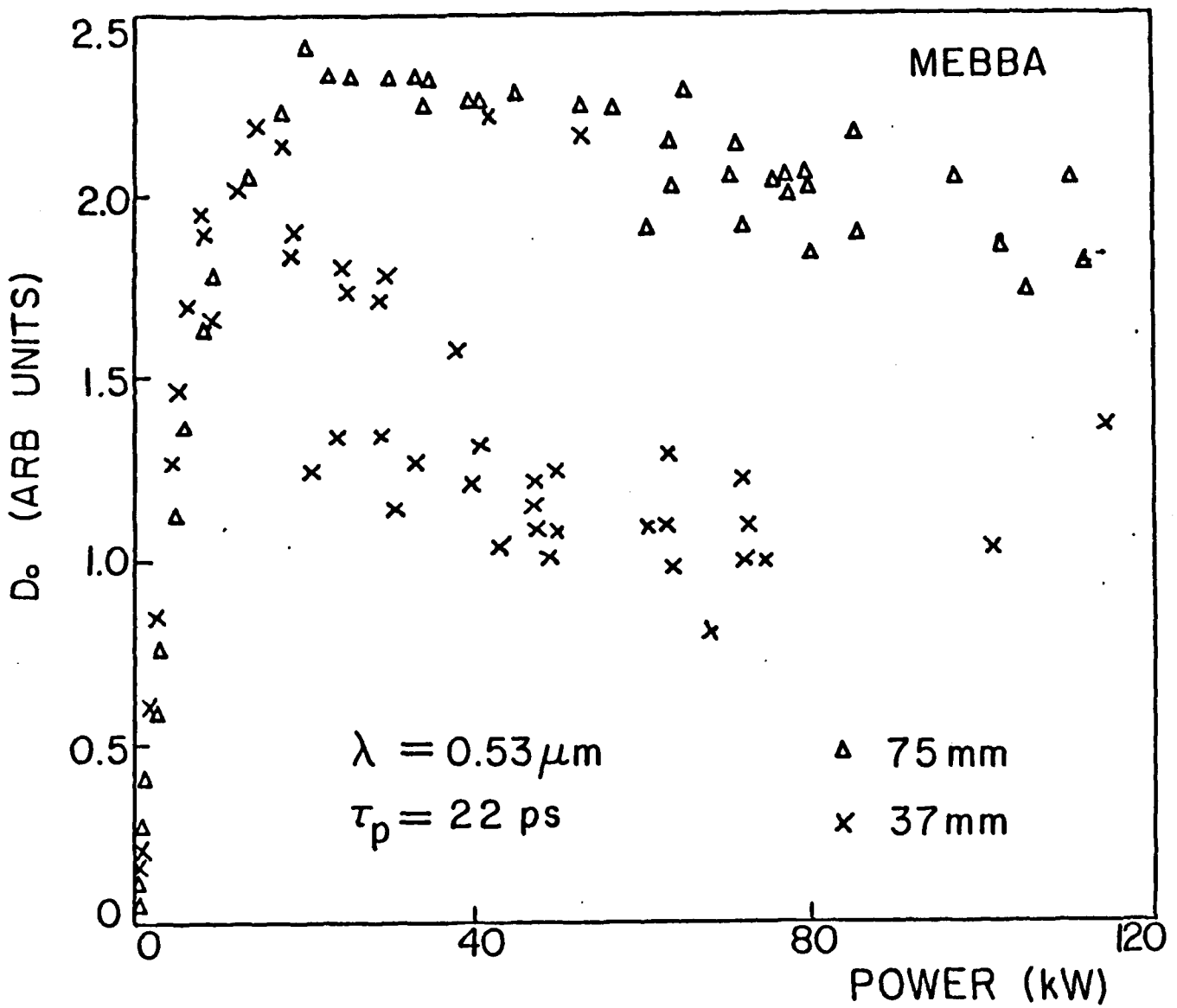
MEBBA
D_o (ARB UNITS)
2.5
2.0
1.5
1.0
0.5
0
0
40
80
120
POWER (kW)
$\lambda = 0.53\mu m$
$\tau_p = 22$ ps
75 mm
37 mm

FIGURE 7

$$\frac{1}{T} \simeq \frac{e^{\alpha L}}{(1-R)^2}\left[1 + \frac{\beta I_0 (1-R)}{\alpha\sqrt{2}}\left(1 - e^{-\alpha L}\right)\right]$$

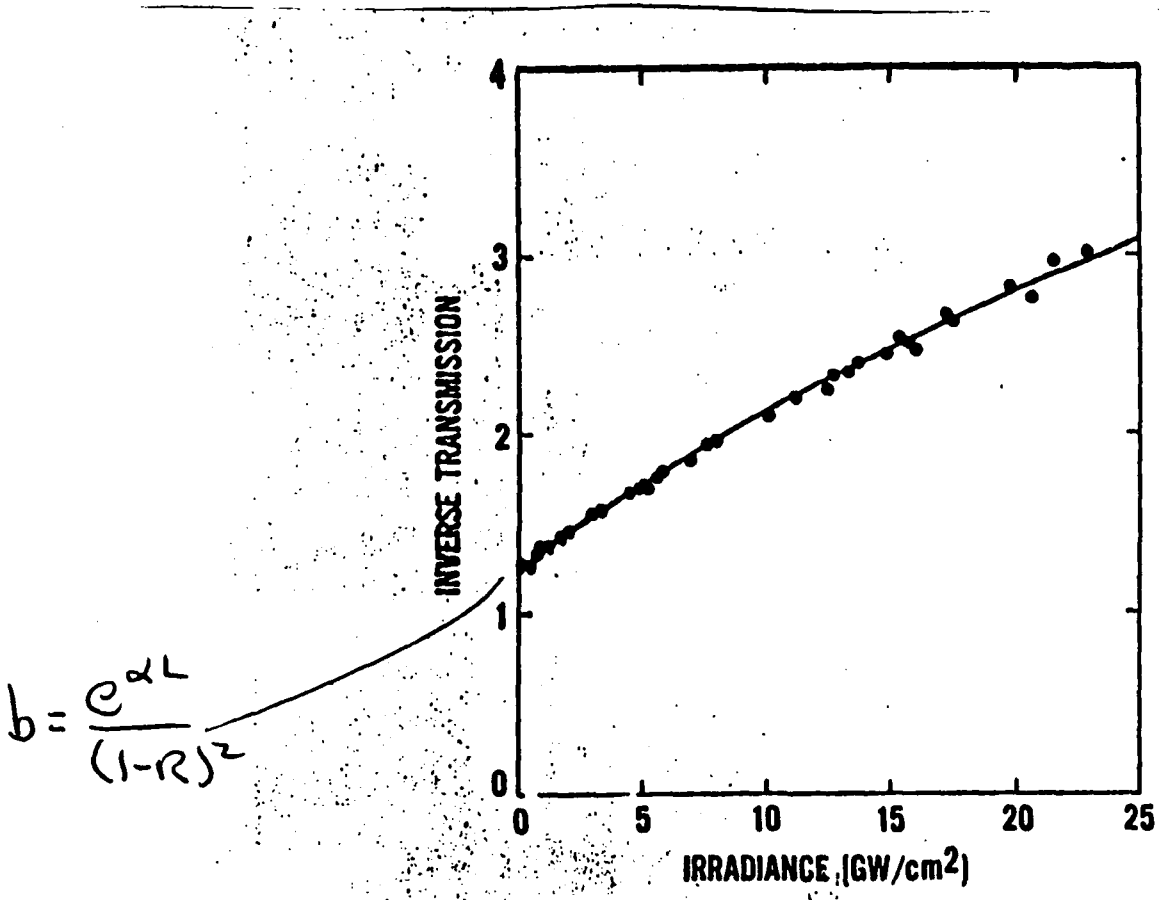

$$b = \frac{e^{\alpha L}}{(1-R)^2}$$

$$y = \frac{e^{\alpha L}\beta\left(1 - e^{-\alpha L}\right)}{\alpha\sqrt{2}\,(1-R)}$$

FIGURE 12 The inverse of the transmission of a 0.5 cm pathlength cell filled with MBBA is plotted as a function of the incident irradiance at 0.53 μm. The solid line is a theoretical fit with a nonlinear absorption coefficient of 0.6 cm/GW.

	CS_2	MBBA	MEBBA
STATE	ISOTROPIC LIQUID	LIQUID CRYSTALS	LIQUID CRYSTALS
DOMINANT EFFECTS	SELF-FOCUSING LASER INDUCED PLASMA	SELF-FOCUSING SCATTERING	SELF-FOCUSING NONLINEAR ABSORPTION
N_2(AT 0.53UM)	1.23×10^{-11} ESU	1.26×10^{-12} ESU	3.9×10^{-11} ESU
THRESHOLD POWER	7.8 KW	80 KW	2.5 KW
PROBLEMS	WELL UNDERSTOOD MATERIAL	NEMATIC AT ROOM TEMP	POSSIBLE DECOMPOSITION COMPLEX ABSORPTION PROCESSES

NEMATIC LIQUID CRYSTALS

MBBA	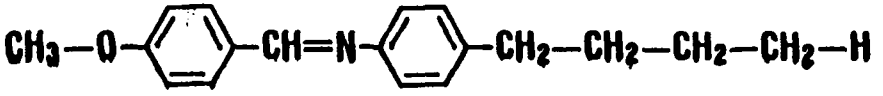	MeOBBuA
MeBBA	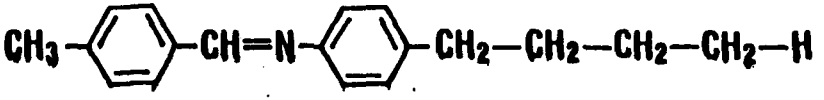	MeBBuA
5-0-1	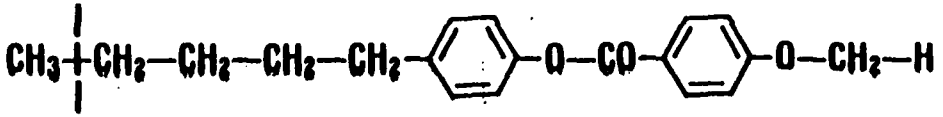	PePMeOB
4-4	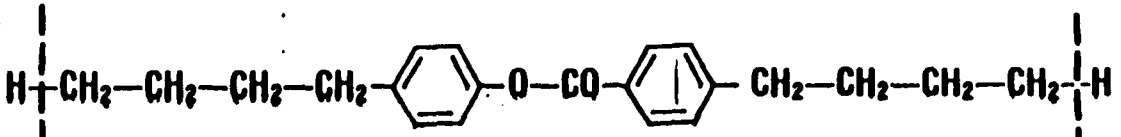	BuPBuB
4-5	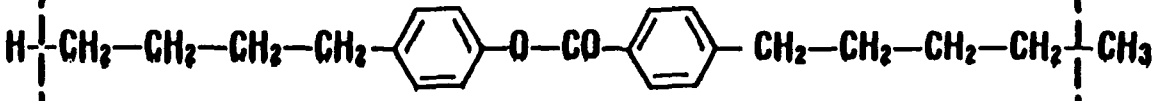	BuPPeB
5-4	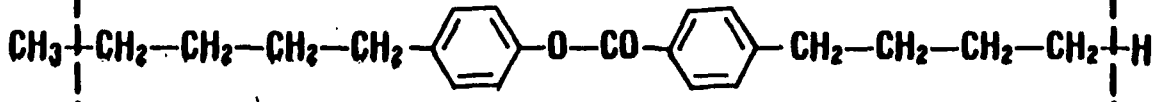	PePBuB
5-5	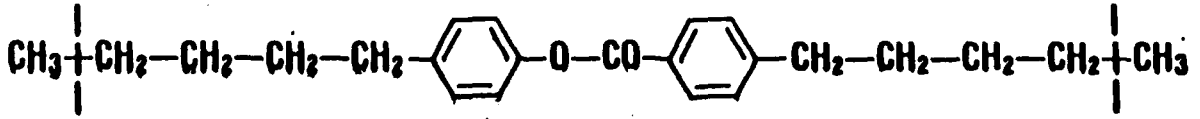	PePPeB

0.53 UM CIRC POL 200 PSEC ETALON

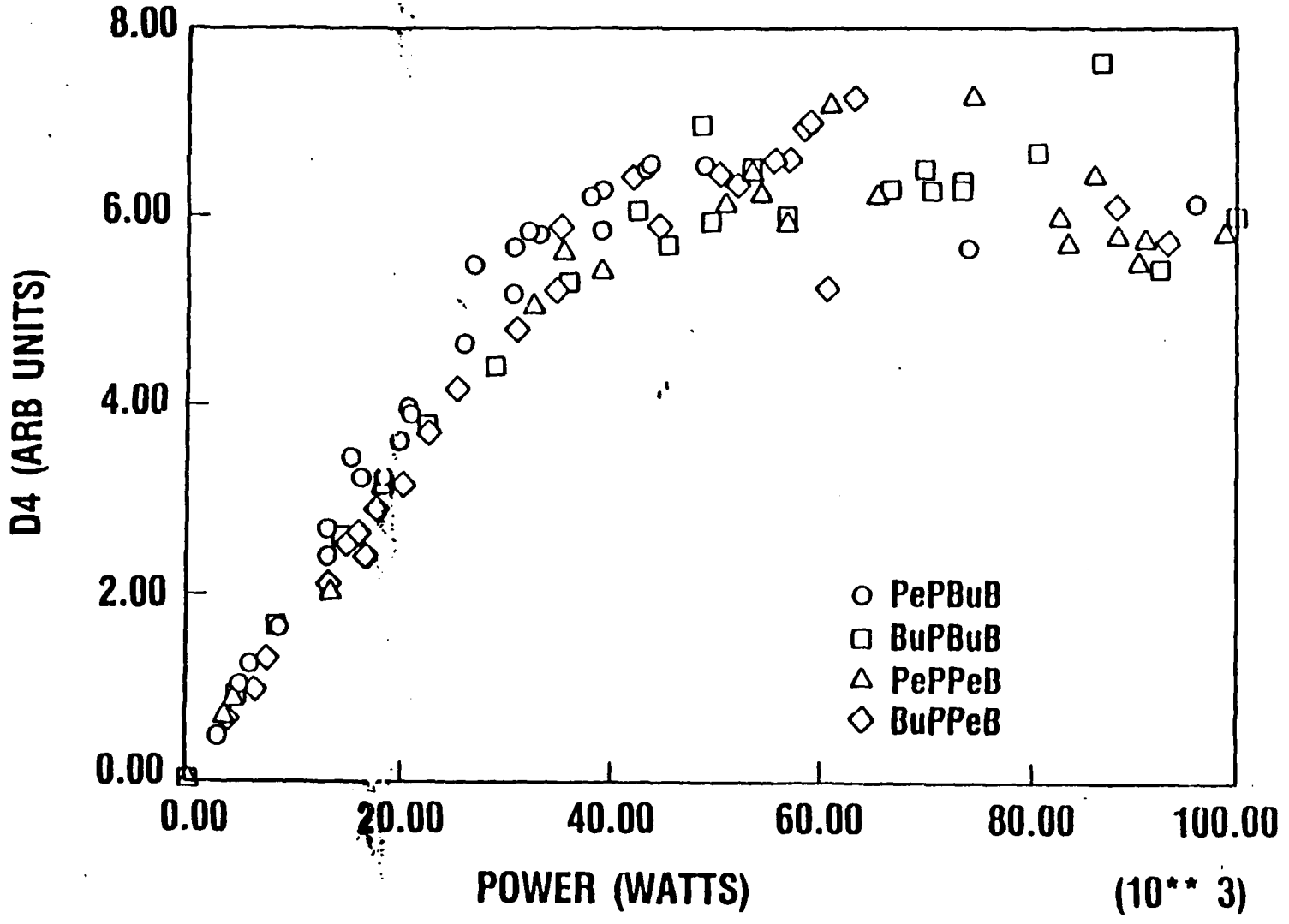

Isomers of Octahedral Chelates

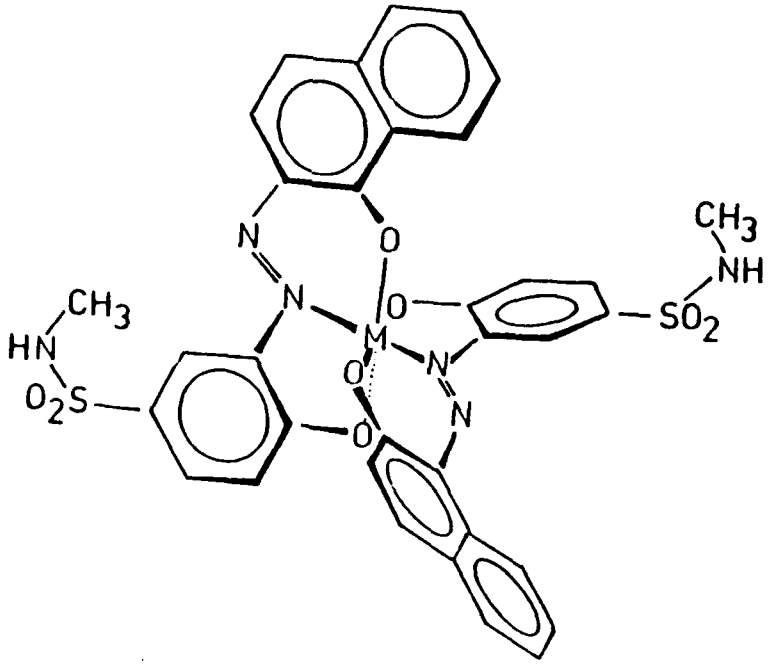

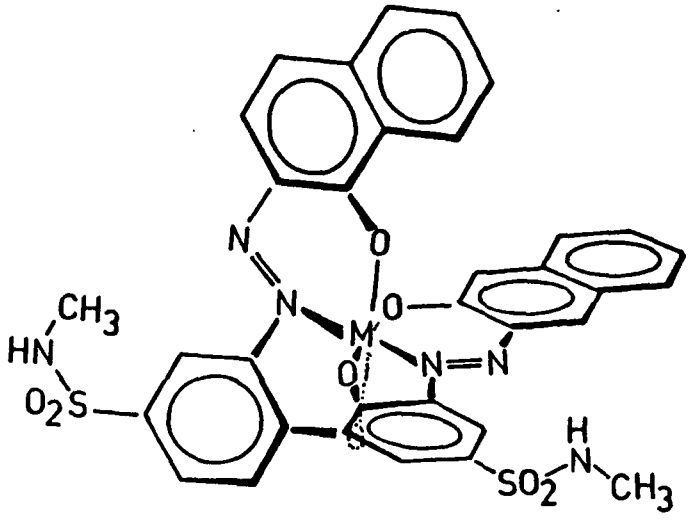

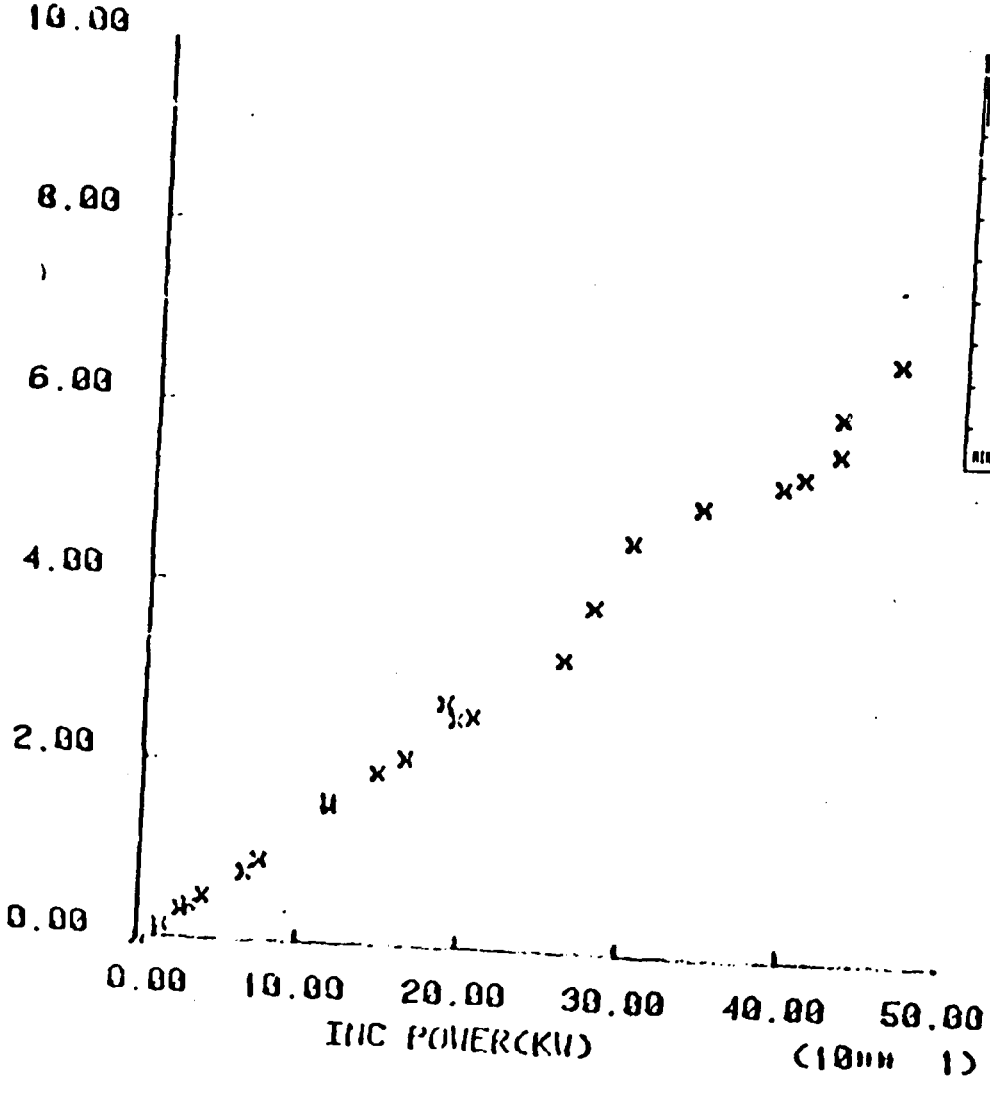
10.00
8.00
6.00
4.00
2.00
0.00
0.00
10.00
20.00
30.00
40.00
50.00
INC POWER(KW)
(10mm 1)

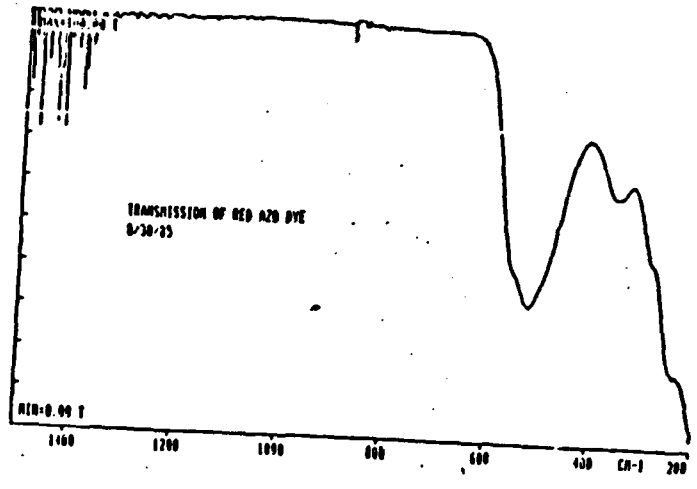
TRANSMISSION OF RED AZO DYE
8/30/85

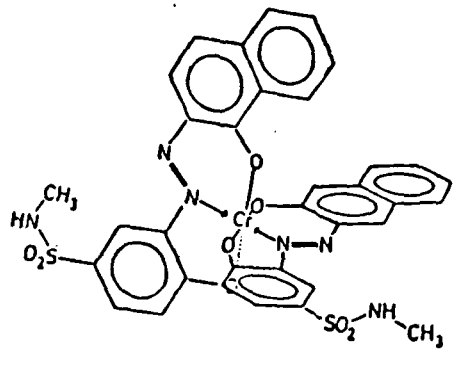
CH3
HN
O2S
N
N
O
Cr
O
O
N
N
SO2
NH
CH3

Square-Planar Chelates

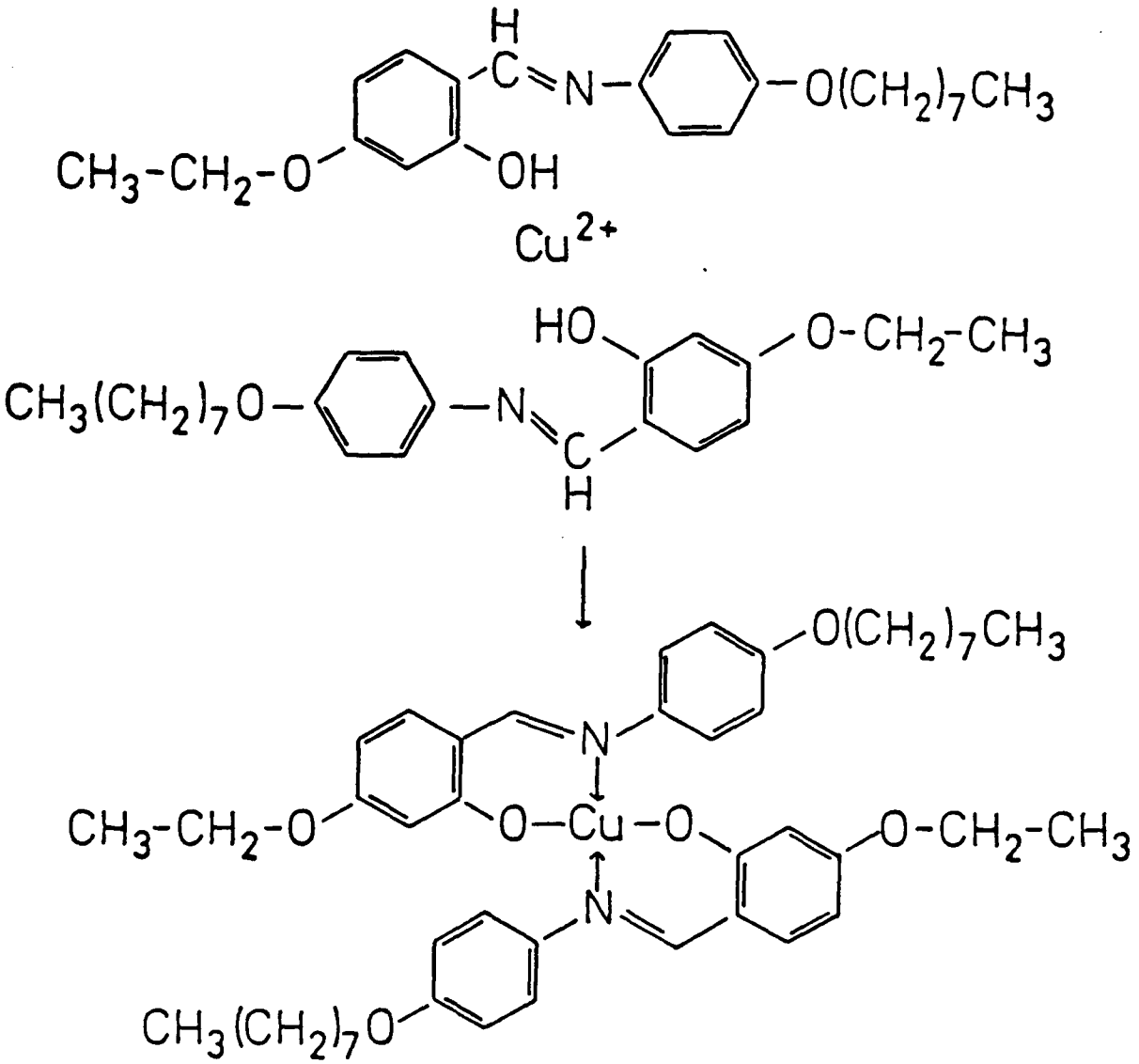

REFERENCES

Mol. Cryst. Liq. Cryst., 1985, Vol. 127, pp. 321–330
0026-8941/85/1274–0321/$15.00/0

Studies of the Nonlinear Switching Properties of Liquid Crystals with Picosecond Pulses

M. J. SOILEAU, SHEKHAR GUHA, WILLIAM E. WILLIAMS, E. W. VAN STRYLAND, and H. VANHERZEELE

Center for Applied Quantum Electronics, Department of Physics, North Texas State University, Denton, Texas 76203

and

J. L. W. POHLMANN, E. J. SHARP, and G. WOOD

Night Vision and Electro-Optics Laboratory, Fort Belvoir, Virginia 22060

(*Received September 6, 1984*)

A comparative study of self-focusing in seven liquid crystals using picosecond 0.53 and 1.06 μm pulses is presented. MEBBA was found to have the highest nonlinearity at 0.53 μm as determined in an optical power limiting experiment. This limiting appears to be due to nonlinear refraction enhanced by two-photon absorption.

We report here the results of a sytematic study of self-focusing in several liquid crystals in the isotropic phase using picosecond pulses at 0.53 μm and 1.06 μm. The samples studied and their chemical compositions are listed in figure 1.

Large nonlinearities have been previously measured in liquid crystals using nanosecond pulses[1] and such materials have been used in cw four-wave mixing experiments.[2] The large nonlinear refractive indices n_2 observed in the earlier work are believed to be due to light induced reorientation of the anisotropic liquid crystal molecules which is a relatively slow process. In order to estimate the value of n_2 in the liquid crystals, a power limiting configuration was used.[3] For highly nonlinear self-focusing materials such as CS_2, it was established in Ref. 3 that the limiting power obtained in such a configura-

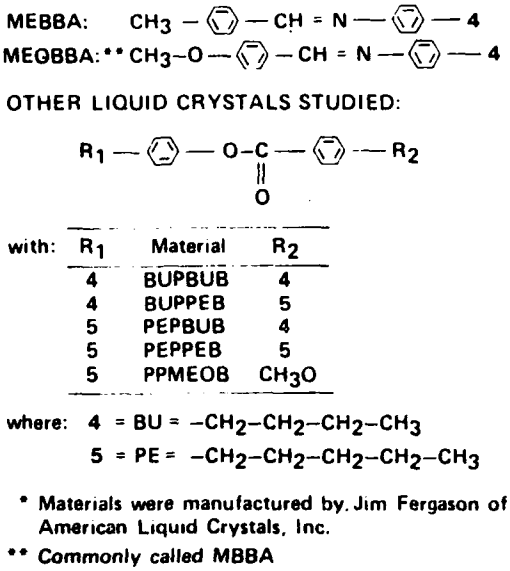

FIGURE 1 Chemical structures and nomenclature for the liquid crystals studied in this work.

tion is P_2, the second critical power for self-focusing. P_2 is related to n_2 by the relation.

$$P_2 = \frac{3.77c\lambda^2}{32\pi^2 n_2} \tag{1}$$

where c is the speed of light in vacuum, λ is the wavelength and 3.77 comes from a numerical solution to the nonlinear wave equation.[4]

The experimental technique is described in detail in Ref. 3 and is summarized here in Fig. 2. A lens (L_1) focuses light from a frequency-doubled mode-locked picosecond Nd:YAG laser operated in the TEM_{00} spatial mode. A second lens (L_2) reimages the transmitted light through an aperture onto the detector D_4 which measures the transmitted energy. As the incident power reaches P_2, the beam undergoes severe phase distortion and the reading on D_4 stops increasing for further increase of input power. This switching is due to self-lensing and subsequent optical breakdown. Figure 3 shows an example of such laser induced switching for CS_2 and MEBBA at 0.53 μm. The input field was linearly polarized. It is to be noted that the switching power for MEBBA is less than that of CS_2.

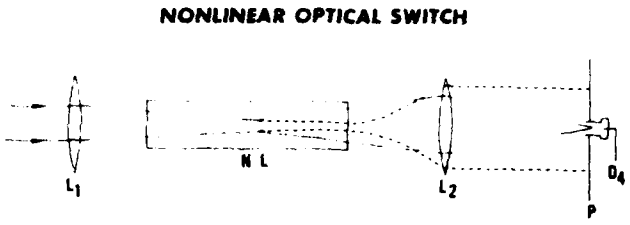

FIGURE 2 Technique for measuring the onset of self-focusing. The solid lines schematically trace the input beam for low input power. The beam is focused into the nonlinear medium by lens L_1 and then imaged by L_2 through an aperture onto detector D_4. The transmission for low input powers can be near unity. As the input power is increased to approximately P_2, the critical power for self-focusing,[1] the beam undergoes severe phase aberrations (i.e., nonlinear refraction) and the transmission through the aperture decreases. The high power situation is shown schematically by the dotted lines.

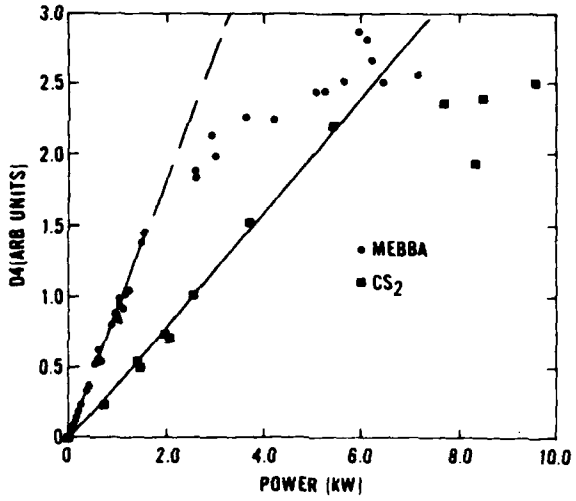

FIGURE 3 Nonlinear optical switching in CS_2 and MEBBA (4-methyl benzylidene 4'-n-butylaniline). The detector reading D_4 monitors the aperture transmission after the sample. D_4 remains unclamped with input power until P_2 is reached. The data shown are for 42 psec (FWHM), linearly polarized 0.53 μm pulses.

The ratio of the critical powers for the circularly polarized field to the linearly polarized field is approximately two for each of the samples studied, as shown in Figs. 4 and 5. Figure 4 shows the switching powers for the liquid crystals MEBBA, MEOBBA (commonly known as MBBA) and PPMEOB for linearly polarized input field and Fig. 5 shows the corresponding results for circularly polarized light. Figures 6 and 7 show the results for linear and circularly

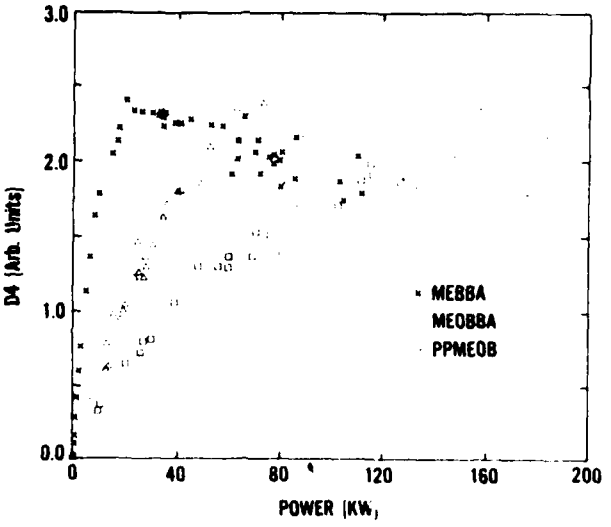

FIGURE 4 Comparison of nonlinear optical switching for the liquid crystals MEBBA, MEOBBA and PPMEOB. Linearly polarized light at 0.53 μm with 42 ps (FWHM) pulsewidth was used.

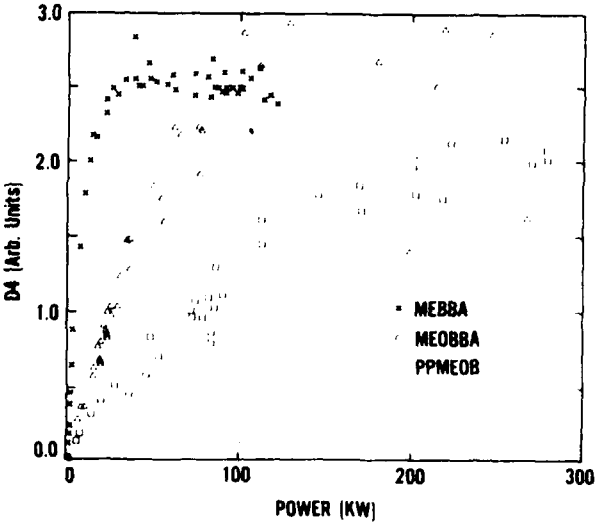

FIGURE 5 Comparison of nonlinear optical switching for the liquid crystals MEBBA, MEOBBA and PPMEOB. Circularly polarized light at 0.53 μm with 42 ps (FWHM) pulsewidth was used.

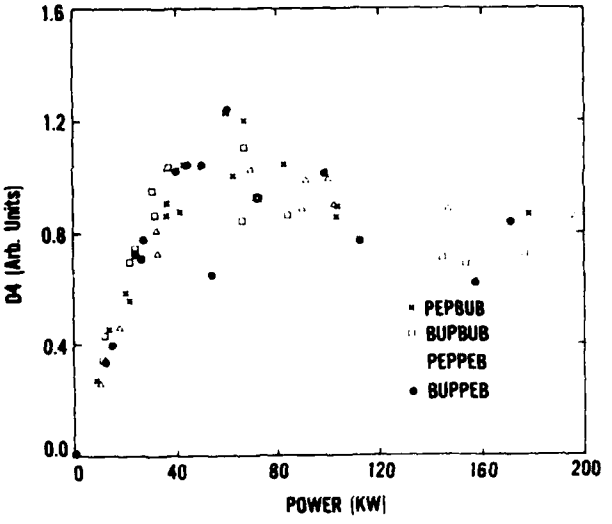

FIGURE 6 Comparison of nonlinear optical switching for the liquid crystals PEPBUB, BUPBUB, PEPPEB and BUPPEB. Linearly polarized light at 0.53 μm with 42 ps (FWHM) pulsewidth was used.

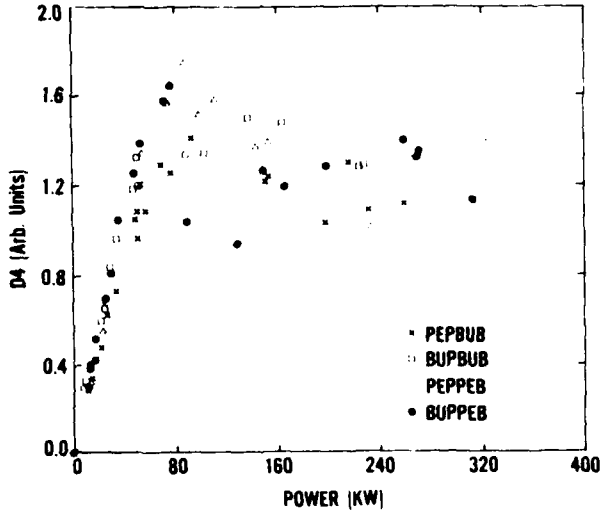

FIGURE 7 Comparison of nonlinear optical switching for the liquid crystals PEPBUB, BUPBUB, PEPPEB and BUPPEB. Circularly polarized light at 0.53 μm with 42 ps (FWHM) pulsewidth was used.

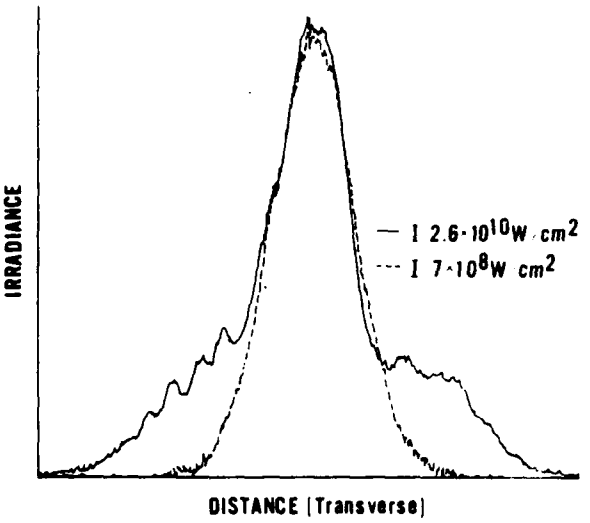

FIGURE 8 Vidicon scans showing the far field spatial profile of a 0.53 μm beam after transmission through an optically thin sample of MEBBA (thickness less than a Rayleigh range). The dashed curve is for low input irradiance and shows no beam distortion. The solid trace is for high irradiance and shows the effects of phase distortion in the sample.

polarized light, respectively, using the liquid crystals PEPBUB, BUPBUB, PEPPEB and BUPPEB. P_2 is seen to have the same value for for each of these four samples and for the sample PPMEOB. The fact that this ratio of switching powers for circular and linear polarizations is two is a clear indication that self-focusing is the dominant mechanism as discussed in Ref. 3. In fact, this is exactly the ratio observed for CS_2 where the dominant nonlinearity is molecular reorientation. Therefore, the observed polarization dependence suggests that the dominant nonlinearity, even for the short pulses, is molecular reorientation for these materials. However, for these large molecules the decay time constant would be expected to be considerably longer than the 42 psec (FWHM) pulses used.

Figure 8 shows the distortion in the far field spatial pattern of the beam after transmission through an optically thin sample of MEBBA (thickness of the sample less than the Rayleigh range). The effect of the optically induced phase distortion is observed by comparing the profiles at high input irradiance (solid curve) to that at low input irradiance (dashed curve). That this phase distortion arises from self-focusing rather than self-defocusing is confirmed by the results

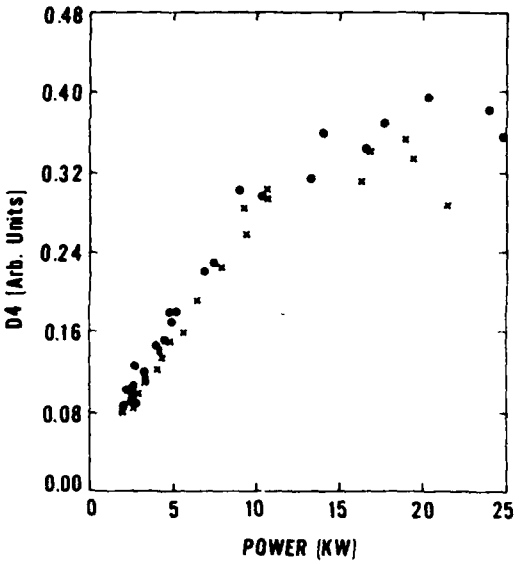

FIGURE 9 Comparison of nonlinear optical switching powers in MEBBA for different input irradiances. The focal length of the lens L_1 was 37.5 mm for the circles and 75 mm for the crosses so that the spot size in the sample changed by a factor of 2 (irradiance changes by 4 for a given power). Linearly polarized light at 0.53 μm with 42 ps (FWHM) was used.

shown in Fig. 9 in which the power dependence of the switching is shown for different input irradiances. The two curves shown correspond to experiments using lenses of focal lengths differing by a factor of two yielding spot sizes differing by a factor of two. If the limiting were due to self-defocusing, a dependence on the input irradiance would be expected, which is seen to be absent in Fig. 9. Also the fact that the switching power remains constant when the irradiance changes by a factor of four shows the dominance of nonlinear refraction as opposed to, for example, nonlinear absorption. An additional indication of self-focusing was the observation that at and above the critical input power there was optical breakdown in the liquid crystal media.

In Fig. 10 a comparison of critical powers in MEBBA at 1.06 μm and 0.53 μm is shown. The ratio of the values of P_2 at the two wavelengths is approximately 20 whereas self-focusing theory only predicts a ratio of 4 between the two wavelengths (see equation 1).[3,4] This large dispersion implies that the mechanism responsible for nonlinear refraction in MEBBA is not simply molecular reorientation.

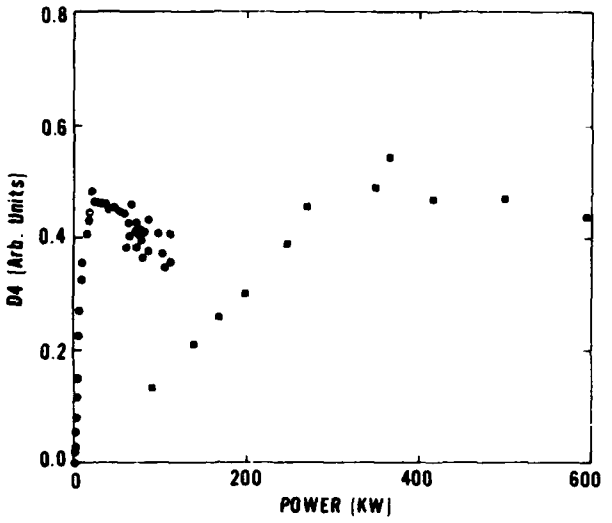

FIGURE 10 Comparison of nonlinear optical switching power in MEBBA between 0.53 μm and 1.06 μm radiation. The pulsewidths used were 42 ps and 67 ps (FWHM) respectively. Linearly polarized light was used.

Figure 11 shows optical switching in PEPBUB, BUPBUB, PEPPEB and BUPPEB at 1.06 μm. Comparing with Fig. 6 we find a ratio of 10 in the critical powers for this set of samples at the two wavelengths. The dispersion is still larger than the prediction of 4 from self-focusing theory, but smaller than that observed in MEBBA.

The larger nonlinearities at 0.53 μm may be due to an enhancement of the nonlinear refraction due to nonlinear absorption. Nonlinear absorption in MEBBA was observed at 0.53 μm and the results are plotted in Fig. 12 where the inverse transmission is displayed as a function of the incident irradiance. The nearly linear dependence on irradiance is consistent with a two-photon absorption process.[5] The dotted line shows the theoretical predictions for a two-photon absorption coefficient of 0.6 ± 0.2 cm/GW. If we now go back to the limiting configuration and calculate, using linear optics, the expected irradiance at focus we find a maximum change of transmission due to two-photon absorption of 15%; not enough by itself to account for the limiting. No nonlinear absorption was observed at 1.06 μm up to irradiances where there was obvious material breakdown. It is worth mentioning that excimer formation by nonlinear absorption of picosecond laser pulses has been observed in liquid benzene[6] and similar processes could play a role in liquid crystals as well.

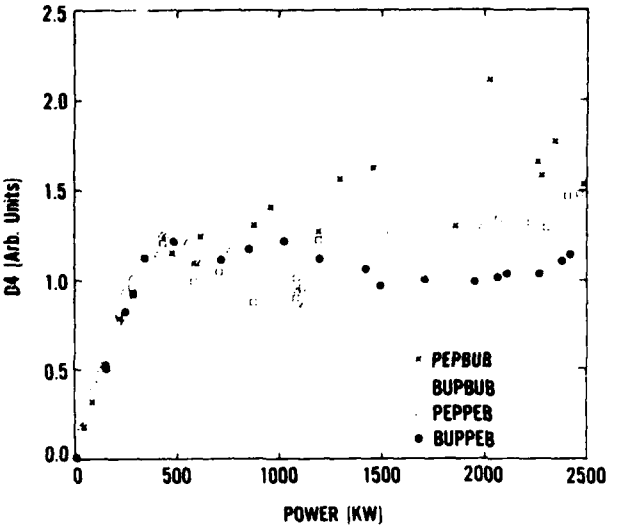

FIGURE 11 Comparison of nonlinear optical switching in PEPBUB, BUPBUB, PEPPEB and BUPPEB at 1.06 μm using linearly polarized light with 67 ps (FWHM) pulsewidth.

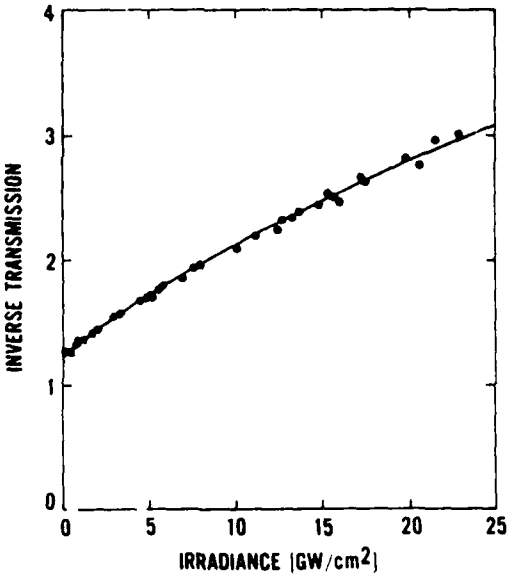

FIGURE 12 The inverse of the transmission of a 0.5 cm pathlength cell filled with MEBBA is plotted as a function of the incident irradiance at 0.53 μm. The solid line is a theoretical fit with a nonlinear absorption coefficient of 0.6 cm/GW.

To summarize, P_2 was measured for various liquid crystals and was found to vary greatly with minor changes in chemical composition. For example the difference between MEBBA and MEOBBA is the addition of a single oxygen atom. The liquid crystals were found to exhibit large and fast nonlinearities comparable to those of the Kerr liquids and are effective materials for optical power limiter applications. In addition, they have potential for applications in the areas of phase conjugation, optical-bistability and optical switching. Extensive studies of nonlinear hyperpolarizabilities of organic molecules have been performed with nanosecond pulses to determine the ways to maximize the nonlinear susceptibility by synthesizing molecules with different substituents.[7] Similar work using liquid crystals and determination of the origins of the nonlinearities would be of practical interest. Further study, including other materials, a determination of the pulsewidth and temperature dependence of the nonlinearities, and a more refined theoretical modeling is currently in progress.

References

1. D. V. G. L. Narashimha Rao and S. Jayaraman, *Appl. Phys. Lett.* **23**, 539 (1973).
2. I. C. Khoo, *Phys. Rev. A* **25**, 1040 (1982).
3. M. J. Soileau, E. W. Williams, and E. W. Van Stryland, *IEEE Journ. Quant. Elec. QE-19* **4**, 731 (1893).
4. J. H. Marburger, *Progress in Quantum Electronics* J. H. Sanders and S. Stenholm, eds., (New York, Pergamon, 1977) pp. 35–110.
5. J. H. Bechtel and W. L. Smith, *Phys. Rev.* **B13**, 3515 (1976).
6. H. Masuhara, H. Miyasaka, N. Ikeda, and N. Mataga, *Chem. Phys. Lett.* **82**, 59 (1981).
7. B. F. Levine and C. G. Bethea, *Journ. Chem. Phys.* **63**, 2666 (1975).

Mol. Cryst. Liq. Cryst., 1987, Vol. 143, pp. 139-143

NONLINEAR OPTICAL PROPERTIES OF LIQUID CRYSTALS IN THE ISOTROPIC PHASE

M. J. SOILEAU, ERIC W. VAN STRYLAND, and SHEKHAR GUHA*
Center for Applied Quantum Electronics, Department of Physics, North Texas State University, Denton, TX 76203
*Present Address: Martin Marietta Laboratories, 1450 South Rolling Road, Baltimore, MD 21227

E. J. SHARP, G. L. WOOD, and J. L. W. POHLMANN
Army Night Vision and Electro-Optics Center, Fort Belvoir, VA 22060-5677

Abstract Picosecond nonlinear absorption and nonlinear refraction were studied for several classes of isotropic phase liquid crystals, including Schiff base and ester compounds. Materials studied exhibit a large two-photon absorption coefficient (β) at 532 nm. Values of β were found to be ~0.6 cm/GW in several of the compounds studied. Nonlinear refraction was also observed and the nonlinear refractive index, n_2 was measured for each material at 1.06 μm using an external self-focusing arrangement. n_2 ranged from 6×10^{-13} esu to 2×10^{-12} esu. The combination of nonlinear absorption and nonlinear refraction in these materials result in optical limiting for input energies as low as 0.15 microjoules for 30 psec pulses at 532 nm.

INTRODUCTION

In this paper we report the results of simple direct measurements of nonlinear absorption and nonlinear refraction in selected liquid crystals in their isotropic phase. These measurements are part of an extensive study of nonlinear optical properties of materials in our laboratories.

I. C. Khoo's invited talk at this meeting[1] contained many excellent examples of the so-called giant optical nonlinearities in liquid crystal materials. These giant nonlinearities are associated with the anisotropy in

the linear susceptibility of these organic molecules and the large scale ordering and changes in structural phase induced by an impressed optical field. These nonlinearities involve large scale motion of the relatively massive liquid crystal molecules and as a result the nonlinear response is quite slow (with response times as large as seconds). Liquid crystals have the delocalized π-electronic structures that have been identified by many workers as potential sources of fast and large optical nonlinearities.[2] In this work we use single pulses of picosecond duration to study such nonlinearities at 532 and 1064 nm. Thermal effects, electrostriction and long time constant reorientational effects are minimized in these measurements and the nonlinearities reported are an upper bound for the fast electronic effects.

EXPERIMENTAL

The laser source for these measurements was a Nd:YAG operated at 1064 nm. This laser system produced output pulses of 30 to 200 psec duration and operated in a single spatial mode (TEM_{00}) as verified by pinhole scans and whole beam analysis with an optical multichannel analyzer. The energy and pulsewidth was monitored for each laser shot using the procedure described in ref. 3. The laser output was harmonically converted to give output at 532 nm. The maximum repetition rate used was 5 Hz, thus insuring that the duty cycle was very low and that thermal effects were minimized.

The measurements were conducted using two very simple techniques which are described in detail elsewhere. In one case the sample thickness is much larger than the depth of focus of the beam (i.e., Rayleigh range) that is tightly focused into the bulk of the material being tested.[4,5] The nonlinear response is monitored by measuring the ratio of the input to the on-axis fluence in the far field of the beam after it exits the sample. This simple technique allows for the rapid comparison of the nonlinear response of many materials. In the case of simple

nonlinearities, such as the electronic Kerr effect, the nonlinear refractive index (n_2) may be extracted from such measurements by monitoring the input power required for the onset of whole beam self-focusing. For more complex nonlinearities we simply determine the input power (P_C) required to limit the far field on-axis fluence. This parameter (P_C) is a rough measure of the combined effects of nonlinear refraction and nonlinear absorption and as such is a good indicator as to whether or not more quantitative measurements should be performed.

In the second technique the Rayleigh range of the beam incident on the sample is larger than the sample thickness and the beam is collimated as it traverses the sample. The two-photon absorption coefficient (β) is determined by measuring the total energy transmitted through the sample as a function of the input irradiance in the manner described in detail in refs. 6 and 7. The nonlinear refractive index (n_2) is determined by measuring the changes in beam shape and/or on-axis fluence in the near or far field of the test cell (see ref. 8 for details).

RESULTS

We have previously reported optical limiting in MBBA (p-methoxy benzylidene p-n-butylanilene).[9] Table I is a summary of P_C, β and n_2 measurements in this material and other liquid crystals of similar structure. All the data shown are for pulsewidths of approximately 30 ps and the liquid crystals were in the isotropic phase. Data for CS_2 are shown for comparison. The data for P_C were taken using the optically thick arrangement described in refs. 4 and 5. P_C is indicative of the total nonlinear response of the materials as previously noted. For simple Kerr nonlinearities P_C is inversely proportional to n_2. Note that P_C at 532 nm is about the same for all the samples tested including CS_2. The P_C (or limiting power) for CS_2 is associated with the onset of whole beam self-focusing whereas the observed limiting in the liquid crystal samples is associated with beam depletion due to two-photon absorption.

The nonlinear refractive index (n_2) was directly measured for these materials using the thin sample arrangement described in ref. 8. Note that in all cases the n_2 values for the liquid crystals are approximately an order of magnitude smaller than that of CS_2.

The relatively low values for the fast nonlinearity (assumed to be due to an optical Kerr effect) measured in these materials is somewhat disappointing considering reports of large, fast nonlinearities in organics reported by other workers. We are in the process of extending our measurements to other organics.

SUMMARY

The two-photon absorption coefficient (β) was measured for five isotropic phase liquid crystals at 532 nm. The values of β are large enough ($\simeq$0.6 cm/GW) for use in various nonlinear optical device applications. The nonlinear refractive index, n_2, was measured at 1064 nm for each sample and was found to be approximately an order of magnitude smaller than that of CS_2. Several other classes of organics were examined at 532 nm and all were found to have a smaller nonlinear response than CS_2.

REFERENCES

1. I. C. Khoo, "Beam Application by Two Wave Mixing with Moving Grating in Liquid Crystals," Proceedings of the International Conference, "Optics of Liquid Crystals," Naples, Italy, July 15-18, 1986.
2. Michael Lee, et al., "Theoretical Determination of Nonlinear Molecular Polarization Using Effective P_i-Electron Hamiltonian," Proceedings of the International Conference, "Optics of Liquid Crystals," Naples, Italy, July 15-18, 1986.
3. Eric W. Van Stryland, M. J. Soileau, Arthur L. Smirl, and William E. Williams, Phys. Rev. B 23, 2144-2151 (1981).
4. M. J. Soileau, William E. Williams, and Eric W. Van Stryland, IEEE J. Quantum Electron QE-19, 731-735 (1983).
5. William E. Williams, M. J. Soileau, and Eric W. Van Stryland, Opt. Commun. 50, 256-260 (1984).
6. Eric W. Van Stryland, H. Vanherzeele, M. A. Woodall, M. J. Soileau, Arthur L. Smirl, Shekhar Guha, and Thomas F. Boggess, Opt. Eng. 24, 613 (1985).

7. Eric W. Van Stryland, M. A. Woodall, H. Vanherzeele, and M. J. Soileau, Opt. Lett. 10, 490-492 (1985).
8. Shekhar Guha, Eric W. Van Stryland, and M. J. Soileau, Opt. Lett. 10, 285-287 (1985).
9. M. J. Soileau, Shekhar Guha, William E. Williams, Eric W. Van Stryland, J. L. W. Pohlmann, E. J. Sharp, and G. Wood, Mol. Cryst. Liq. Cryst. 127, 321-330 (1984).

TABLE I

The molecular structure of the samples studied are of the form:

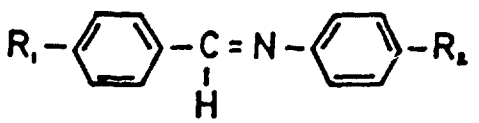

Sample	Color	R_1	R_2	P_C(kW) at 532 nm	(cm/GW) at 532 nm	$n_2 \times 10^{13}$(esu) at 1064 nm
MEBBA	Orange	CH_3	C_4H_9	7±1	.55±.05	6±1
ETBBA	Light Yellow	C_2H_5	C_4H_9	8±1	.5 ±.05	17±2
IPBBA	Light Yellow	C_3H_7	C_4H_9	8±1	.5 ±.05	13±2
BBIPA	Orange	C_4H_9	C_3H_7	7±1	.5 ±.05	12±2
PEBBA	Orange	C_5H_{11}	C_4H_9	7±1	.55±.05	14±2
CS_2	Clear			8±1	Small	130

LIST OF ATTENDEES

5. LIST OF ATTENDEES

FEMTOSECOND TIME-RESOLVED SPECTROSCOPY

November 8, 1988

NAME	AFFILIATION
Ron Antos	University of Rochester
Bill Clark	NVEOC
Brian Monson	NVEOC/University of Arkansas
Greg Salamo	NVEOC/University of Arkansas
Edward Sharp	NVEOC
Ian Walmsley	University of Rochester
Gary L. Wood	NVEOC